Nanoparticle Labels in Bioaffinity Assays

by

Antti Valanne

Logic is a system whereby one may go wrong with confidence.
– Charles F. Kettering

Contents

List of Original Publications

The thesis is based on the following publications, referred to in text by their Roman numerals.

I   Antti Valanne, Saila Huopalahti, Tero Soukka, Raija Vainionpää, Timo Lövgren, Harri Härmä (2005). A sensitive adenovirus immunoassay as a model for using nanoparticle label technology in virus diagnostics. J Clin Virol 33: 217-223.

II   Antti Valanne, Saila Huopalahti, Raija Vainionpää, Timo Lövgren, Harri Härmä (2005). Rapid and sensitive HBsAg immunoassay based on fluorescent nanoparticle labels and time-resolved detection. J Virol Methods 129: 83-90.

III   Antti Valanne, Hanne Lindroos, Timo Lövgren, Tero Soukka (2005). A novel homogeneous assay format utilising proximity dependent fluorescence energy transfer between particulate labels. Anal Chim Acta 539: 251-256.

IV   Antti Valanne, Päivi Malmi, Heidi Appelblom, Pauliina Niemelä, Tero Soukka (2008). A dual-step fluorescence resonance energy transfer-based quenching assay for screening of caspase-3 inhibitors. Anal Biochem 375: 71-81.

V   Antti Valanne, Janne Suojanen, Jouko Peltonen, Tero Soukka, Pekka Hänninen, Harri Härmä (2009). Multiple sized europium(III)-chelate-dyed polystyrene particles as donors in FRET – an application for sensitive protein quantification utilizing competitive adsorption. Manuscript submitted.

The original publications have been reproduced with permission from the copyright holders.

Abbreviations

AF680	Alexa Fluor™ 680
BBQ650	BlackBerry quencher 650
BSA	Bovine serum albumin
BSA-AF	BSA modified with Alexa Fluor™ 680
DTT	Dithiothreitol
EDC	1-ethyl-3-(3-dimethylaminopropyl) carbodiimide hydrochloride
EIA	Enzyme immunoassay
ELISA	Enzyme-linked immunosorbent assay
FIA	Fluoroimmunoassay
FRET	Fluorescence resonance energy transfer
HBsAg	Hepatitis B surface antigen
IFMA	Immunofluorometric assay
IR	Infrared
LLD	Lowest limit of detection
LOCI	Luminescent oxygen channeling assay
NHS	N-hydroxysuccinimide
NTA	Nitrilotriacetic acid
PCR	Polymerase chain reaction
PSA	Prostate-specific antigen
SPA	Scintillation proximity assay
TR-IFMA	Time-resolved immunofluorometric assay
UCP	Up-converting phosphor
UV	Ultraviolet

Abstract

Nanoparticles offer adjustable and expandable reactive surface area compared to the more traditional solid phase forms utilized in bioaffinity assays due to the high surface-to-volume ratio. The versatility of nanoparticles is further improved by the ability to incorporate various molecular complexes such as luminophores into the core. Nanoparticle labels composed of polystyrene, silica, inorganic crystals doped with high number of luminophores, preferably lanthanide(III) complexes, are employed in bioaffinity assays. Other label species such as semiconductor crystals (quantum dots) or colloidal gold clusters are also utilized. The surface derivatization of such particles with biomolecules is crucial for the applicability to bioaffinity assays. The effectiveness of a coating is reliant on the biomolecule and particle surface characteristics and the selected coupling technique. The most critical aspects of the particle labels in bioaffinity assays are their size-dependent features. For polystyrene, silica and inorganic phosphor particles, these include the kinetics, specific activity and colloidal stability. For quantum dots and gold colloids, the spectral properties are also dependent on particle size.

This study reports the utilization of europium(III)-chelate-embedded nanoparticle labels in the development of bioaffinity assays. The experimental covers both the heterogeneous and homogeneous assay formats elucidating the wide applicability of the nanoparticles. It was revealed that the employment of europium(III) nanoparticles in heterogeneous assays for viral antigens, adenovirus hexon and hepatitis B surface antigen (HBsAg), resulted in sensitivity improvement of 10-1000 fold compared to the reference methods. This improvement was attributed to the extreme specific activity and enhanced monovalent affinity of the nanoparticles conjugates. The applicability of europium(III)-chelate-doped nanoparticles to homogeneous assay formats were proved in two completely different experimental settings; assays based on immunological recognition or proteolytic activity. It was shown that in addition to small molecule acceptors, particulate acceptors may also be employed due to the high specific activity of the particles promoting proximity-induced reabsorptive energy transfer in addition to non-radiative energy transfer. The principle of proteolytic activity assay relied on a novel dual-step FRET concept, wherein the streptavidin-derivatized europium(III)-chelate-doped nanoparticles were used as donors for peptide substrates modified with biotin and terminal europium emission compliant primary acceptor and a secondary quencher acceptor. The recorded sensitized emission was proportional to the enzyme activity, and the assay response to various inhibitor doses was in agreement with those found in literature showing the feasibility of the technique. Experiments regarding the impact of donor particle size on the extent of direct donor fluorescence and reabsorptive excitation interference in a FRET-based application was conducted with differently sized europium(III)-chelate-doped nanoparticles. It was shown that the size effect was minimal.

1   Introduction

The early days of bioaffinity assays go back to the 60's, when the realization of the first methods benefiting from radiolabelled reporter molecules and competitive assay formats took place (Berson & Yalow, 1959; Ekins, 1960). Also, non-competitive or two-site immunoassays were introduced already in the late 1960s by Wide et al. (1967) and Miles & Hales (1968), which enabled higher sensitivity potential (Kricka 1994; Ekins 1987; Davies 2001) compared to that of the competitive principle. Since then, various aspects of assays in general have been tuned to meet the requirements of the evolving knowledge around the myriad of biomolecules, novel label technologies and practical aspects of diagnostic laboratory work. Radiolabels, the reporter molecules still extensively used in bioaffinity assays have been replaced by non-isotopic alternatives due to the environmental and economic disadvantages associated with hazardous radioactivity and the drive for greater assay sensitivity and multianalyte assays (Ekins & Chu 1994). The concept of sensitivity has been debated in the insightful report of Ekins (1997). Not only the assay principles, but also the non-isotopic enzyme- and luminescent labels, new detection technologies, their limitations and potentials have been delved into in numerous fundamental studies (Ekins & Dakubu 1985; Hemmilä et al. 1984; Soini & Lövgren 1987). Photoluminescent labels, i.e. luminophores excitable with photons are currently the predominant alternative to displace radiolabels, although they are not without disadvantages This has been mainly associated with autofluorescence, a property of biological material, plastic ware and poor quality optics to emit short-lived fluorescence upon high energy excitation, which may impair the assay sensitivity. In this regard, phycobiliproteins with higher quantum yields or more efficient absorptivity have been studied (Grabowski et al. 1978; Oi et al. 1982). Also, cyanine dyes excitable at visible or near-infrared wavelengths, at which biological materials are nearly transparent, have been experimented (Ernst et al. 1989). However, after the discovery of fluorophores exhibiting long lifetime fluorescence, i.e. lanthanide(III) chelates (Leif et al. 1977; Soini & Hemmilä 1979; Evangelista et al. 1988; Diamandis 1990; Hemmilä et al. 1984; Hemmilä 1988; Soini & Kojola 1983), cryptates (Lehn 1978; Prat et al. 1991) or crystals (Tanke et al. 1986; Beverloo et al. 1990), the effective elimination of autofluorescence was achieved. Also, bioluminescent and chemiluminescent labels, i.e. luminescence induced by a biomolecular or chemical reaction, respectively, have been employed in diagnostics (see reviews of Boekx (1984) and Seitz (1984)). Despite the lack of autofluorescence and improved biocompatibility of these techniques compared to photoluminescent techniques overall, these assays are more complex to conduct because of the additional signal generation step and reaction components.

Currently the most sensitive and clinically most valuable techniques applied in routine diagnostics rely on immunoreactions, where the biomolecules (or analytes)

of interest are captured and quantified by antibodies. The prime examples of assay techniques relying on immunorecognition are ELISA/EIA (enzyme-linked immunosorbent assay/enzyme immunoassay) (Engvall & Perlmann 1971;van Weemen & Schuurs 1971), IFMA (immunofluorometric assay, non-competitive format) and FIA (fluoroimmunoassay, competitive format) type assays (Hemmilä 1985). Therefore, the development of monoclonal antibodies was a sensational hallmark (Kohler & Milstein 1975). In addition to the development of the heterogeneous (or separation-based) assay formats, homogeneous (or separation-free) assays were developed later to shorten the turnaround time of a single analysis. Methods like scintillation proximity assay (SPA) (Hart & Greenwald 1979), luminescent oxygen channelling assay (LOCI) (Ullman et al. 1996) and techniques based on fluorescence polarization (Perrin 1926), fluorescence (or Förster) resonance energy transfer (FRET) (Förster 1948) and fluorescence correlation spectroscopy (Ehrenberg & Rigler 1974; Elson & Magde 1974) enabled detection of molecular interactions without the need for a washing step. This development led to the establishment of a new application field of rapid molecular screening employed in e.g. drug discovery, where high measurement capacity was the highest priority. The 'mix-and-measure' ideology was established to ensure the automation was technologically feasible and cost-effective, and that the assay throughput did not become a bottleneck for the screening of massive compound libraries (Broach & Thorner 1996). In conjunction with the high-throughput technologies, the development of point-of-care type diagnostic assays, i.e. assays conducted during the patient visit, which provide rapid turnaround times but do not require high measurement capacity, has formed another branch of modern assay development (Rowe et al. 1999; Plowman et al. 1999; Schult et al. 1999; Bernard et al. 2001; von Lode et al. 2003, 2004). Previously, the need for quantitative results of high sensitivity and specificity, comparable to the well established central laboratory assays, has been focused on in the forefront of point-of-care test development (Ahn et al. 2003; von Lode et al. 2004). Overall, the desire for improved assay performance, including high sensitivity and broad dynamic range (the linear range of dose-response curve), in the field of drug discovery and diagnostics has led to search for better instrumentation, molecular binders with higher specificity and affinity and alternative label technologies. This is where the potential of various particulate labels has been experimented.

2   Review of the Literature

The first bioaffinity assays utilizing particles originate to the 1950s, when the invention
of latex agglutination tests took place (Singer & Plotz 1956). At that time the particle
size was in micrometer range, but gradually, the size has decreased to nanometer scale.
Important advantages of particles compared to a conventional solid phase (e.g. filter
membrane or microtiter plate well) is their mobility leading to enhanced reaction kinetics,
and the expanded and fully adjustable reactive surface area. The applicability of particles is
further improved by the ability to modify the surface characteristics and the incorporation
of different label molecules. Particulate labels brought the concept of true high specific
activity into the scene of non-isotopic bioaffinity assays. This was accompanied by other
labelling techniques aiming at high specific activity, e.g. the introduction of multiple
labels conjugated directly or indirectly by a carrier to a molecule of choice (Kricka 1993;
Kricka 1996) or PCR-based amplification of label signal (Saito et al. 1999). A variety of
particulate materials doped with label molecules, polymeric organic or inorganic lattices
including latex particles, lanthanide(III) crystals, upconverting phosphors, quantum dots
and gold colloids, has been employed as labels in bioaffinity assays. The specific activity,
which is adjustable by the label character and dose or by the lattice composition or size,
and the enhanced binding capacity are the main assets inherent to labelled particles
coated with binding molecules. On the other hand, particle size-dependent luminescent
properties are specific for extremely small particles like quantum dots and gold colloids.
These aspects are utilizable in both heterogeneous and homogeneous assay formats, but
the requirements and preferences for either principle feature distinctions from one another.
In addition to particulate reporters, this review focuses on aspects regarding surfaces and
functionalization of various forms of photoluminescent particles and discusses their impact
on both heterogeneous and homogeneous bioaffinity assays. This discussion is targeted to
particle sizes of 2 to 200 nm in diameter.

2.1   Features of particulate labels

Particulate labels can be defined as inorganic or organic polymeric entities of mostly uniform
shape and size, which incorporate a multitude of molecules, ions or atoms quantifiable
using an established detection technology. Most commonly particle labels are detected by
their luminescence, the induction of which the composition of incorporated luminophores
dictates. As a principal interest, particulate labels were developed as a means to couple a
high number of label molecules to molecular binders used in bioaffinity assays. This was
a part of the progression to develop assays of higher sensitivity (Kricka 1993, 1994, 1996)
for clinically important biomarkers. Assays relying on particulate labels usually require
the possibility to conjugate binding molecules onto the surface of the particle, a properly

selected particle size to ensure recognition of the binding molecule and suitable kinetics, and the compatibility of the prepared particle surface with assay reagents and matrices. The last aspect is mostly related to non-specific interactions of the particles with other system components including molecules and solid surfaces. The non-specific interaction is an important aspect regarding the applicability of particles given the concept of high specific activity. The benefit of a particle label coated with binding molecules compared to a soluble counterpart, for instance a labelled antibody, is that the affinity of the binder is not affected by a chemical modification. This means that a high number of labels, the extent mostly reliant on the particle size, can be conjugated to a single binding molecule without altering its chemical composition deliberately. This, in turn, could culminate into a loss of natural activity or increased non-specific binding (Laukkanen et al. 1995) of the binding molecule. The particulate shell does not only function as a physical barrier to define the outline of an individual unit, or as the interface for molecule attachment, it also protects the particle contents from variations of external conditions (Ye et al. 2004) This is particularly true in the case inorganic phosphors and quantum dots, for which a protective layer is essential, but also for the chelate-dyed polymeric latex particles (Kokko et al. 2007). In essence, the chemical moieties such as luminophores incorporated beneath the particle shell must be in a specific environment to exhibit the inherent quantum properties as efficiently as possible. The ability of the shell to repel environmental effects that could modulate the yield of the quantifiable units, e.g. photons, emitted by the particles is considered mostly beneficial for the applicability of the labels. Therefore, the particulate labels are usually considered as more robust than conventional labels, whose quantum properties or structural integrity are prone to change with environmental alterations such as pH-value, ionic strength, or interferences caused by other molecules.

2.2   Luminescent particles

Conventional luminophores feature an inner filter effect or self-quenching when excited at high concentration. This phenomenon stems from the close proximity of individual luminophores and small Stokes' shift determined as the difference of the maximum excitation and emission wavelengths. This, in turn, is a consequence of energetically small internal conversion, i.e. the singlet emission transfer states being energetically close to the singlet excitation state of the electrons. The electronic transition regarding luminescence occurring through this phenomenon called down-conversion is illustrated in Figure 1. For most conventional labels, the down-conversion is minimal, or the excitation and emission spectra overlap (Fig. 2), and therefore, the luminophore concentration in particle doping has to be adjusted carefully not to cause self-quenching (Hemmilä 1985). Owing to this limitation, the number of conventional fluorophores per particulate volume (nm^3) is around 0.01 as assessed by Haugland (1995). Arrays of particles doped with conventional fluorophores are commercially available with a variety of size and surface

modifications, and numerous bioaffinity applications utilizing the detection of such particles have been reported (Irvine et al. 2002; Romero-Steiner et al. 2006; Tocchetti et al. 2001; Wang et al. 2001). Another particle type called TransFluoSpheres™ (Molecular Probes Inc., Invitrogen, OR), is a series of fluorescent particles combining multiple conventional fluorophore species in one unit (Roberts et al. 1998). Using these particles, the internal FRET-relay upon excitation and an apparent broadening of the Stokes' shift are properties that facilitate the fine-tuning of the emission and excitation wavelengths. The benefit of particle labels doped with conventional fluorophores is, however, restricted by the limited specific activity. Therefore, this review focuses on other particle types, with the emphasis on lanthanide(III) particles of various forms because of their better applicability in the field of bioaffinity assays. Also quantum dots and gold colloids are introduced due to their extraordinary properties.
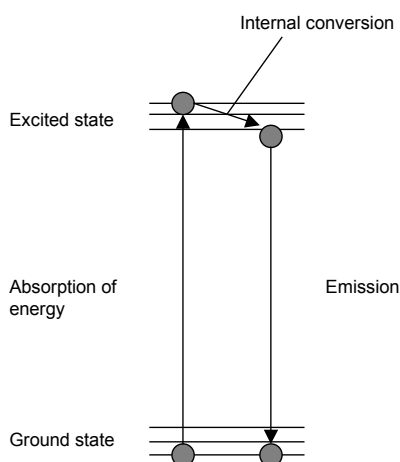
Figure 1. Electronic transitions occurring in fluorescence. The energy loss upon internal conversion translates into emission of lower energy than required for the excitation.
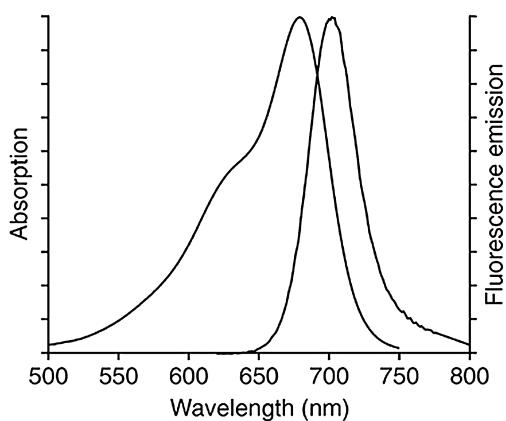
Figure 2. The excitation and emission spectra of a conventional fluorophore (Alexa Fluor™ 680 by Molecular Probes Inc.).

Photoluminescent lanthanide(III) chelates, cryptates or inorganic lattices in general feature large down-conversions of the excitation light (i.e. large Stokes' shifts), which eliminate the concentration-bound restriction with respect to self-quenching (Diamandis 1992). Therefore, the number of such luminophores per nm^3 of particulate volume can be 100-fold higher (Härmä et al. 2001) than that of the particles impregnated with conventional fluorophores described above. As for the lanthanide(III) chelates or cryptates, the broad Stokes' shift is partly due to the energy loss upon intersystem crossing resulting from an electron spin flip into a lower triplet energy state of the e.g. chelate or cryptate. Further energy is lost when the energy of the triplet state is rapidly transferred to the co-ordinated lanthanide ion. The phenomena are illustrated in Figure 3. The emission characteristics of inorganic lattices doped with lanthanides show similar traits as the chelated lanthanides, only the excitation is usually of higher energy due to the crystal lattice augmenting the excitation of the ion instead of an organic antenna. The most prominent lanthanides in down-converting complexes are europium (Eu), terbium (Tb), samarium (Sm) and dysprosium (Dy). Owing to the large down-conversion, the specific activity of the particles incorporating lanthanide(III) complexes is mostly limited by the concentration of the doped complex and the size of an individual particle. Lanthanide(III) complexes possess long emission decays from microseconds to milliseconds enabling time-resolved measurements (Diamandis 1991). This means that the photon counting window of a fluorometer need not to be opened earlier than several microseconds after the excitation pulse. The elimination of short-lived autofluorescence emanating from biological assay components and matrices is a great contributor to the higher signal-to-background ratio (Frank & Sundberg 1981a, 1981b), and in turn, higher assay sensitivity. This technique is called time-resolved fluorometry (Ekins & Dakubu 1985; Soini & Lövgren 1987; Hemmilä 1988). Lanthanide(III) complexes exhibit narrow emission peaks (peak width ~10 nm) (Fig. 4) compared to conventional fluorophores, which usually feature mirror image overlapping excitation and emission spectra with relatively broad peaks (peak width of ~50 nm) as illustrated in Figure 2. However, in addition to the main emission peak, multiple secondary peaks are inherent to lanthanide luminescence (Fig. 4) due to multiple energetically distinct radiative transitions of the electrons from the excited to ground state. The secondary emission wavelengths, or in the special cases some non-radiative relaxation transitions from higher energy levels (Laitala & Hemmilä, 2005), can also be exploited in assays, but they are more commonly utilized in (F) RET-based applications, where lanthanide(III) complexes are employed as donors. Further advantage compared to the conventional fluorophores is that lanthanide(III) complexes, especially the lanthanide crystals possess higher photostability due to the lack of organic structure susceptible to excitation light disintegration. Lanthanide(III) complex-doped particles are mostly composed of polystyrene or inorganic compounds such as silica or crystal forming salts. Also liposomal assemblies impregnated with

lanthanide(III) complexes have been prepared and utilized successfully (Roy et al. 2003; Laukkanen et al. 1995). Polystyrene and silica are moderately easy to modify to reach the desired size and surface characteristics, though the disadvantage of polystyrene particles is that they may be susceptible to swelling, dye leaking and agglomeration (Santra et al. 2001). They are also large in size, mostly > 50 nm in diameter, which may be problematic due to potential steric and kinetic issues in specific applications. On the other hand, generally smaller and more hydrophilic particles composed of silica networks are susceptible to dissolution in alkaline conditions (Paik et al. 2001), which reduces the overall applicability of the particulate silica. Inorganic lanthanide(III) crystals are typically small in size but they must be capped by a surface layer to render them hydrophilic and accepting for biomolecule conjugation (Beverloo et al. 1992). Thus the preparation of functional crystals is always more labor-intensive and prone to variations (Feng et al. 2003). Furthermore, the excitation of the lanthanide(III) crystals is often at higher energy than that of the chelates, which may introduce higher instrument background (Soukka et al. 2005) and be disruptive to biological samples (Beverloo et al. 1992). Also, the quantum efficiency is decreased when the crystal size is decreased below 500 nm in diameter due to quenching processes at the particle surface (Beverloo et al. 1992).
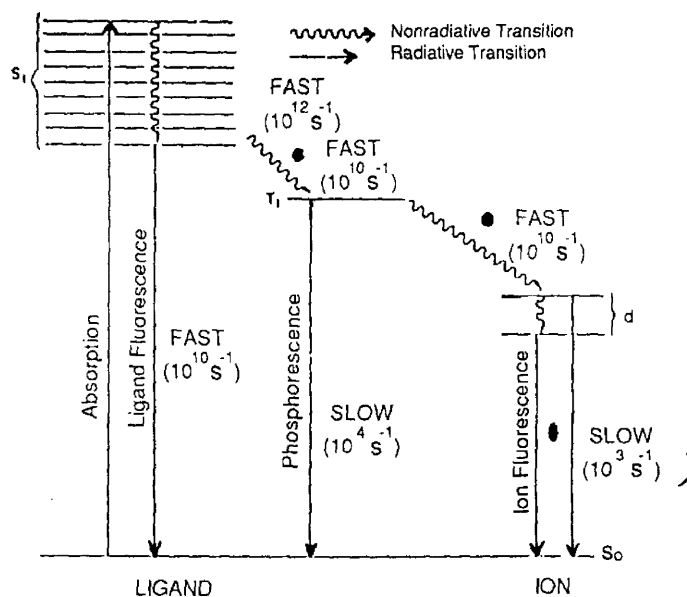
Figure 3. An illustration of the electronic transitions occurring in chelated or cryptated lanthanide(III) complexes. The excitation light is first absorbed by the chelate or cryptate, here designated as 'ligand', followed by a rapid non-radiative internal conversion and intersystem crossing into the triplet state. From this excitation state, the chelate transfers energy to the lanthanide ion, whose relaxation into the ground state commences through radiative transition, i.e. fluorescence. Since the relaxation of the ion is slow, the observed fluorescence of the lanthanide is long-lived (Diamandis 1988).
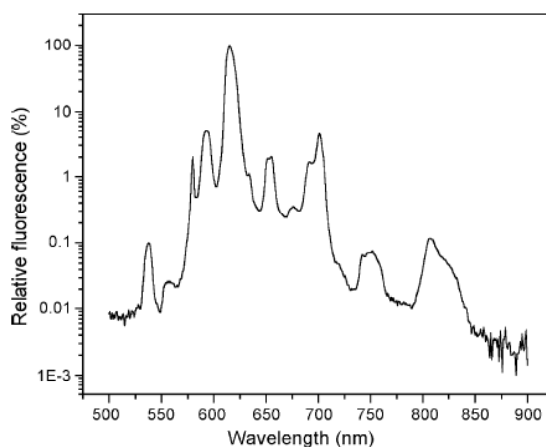
Figure 4. The emission spectrum of chelated (beta-diketone) europium(III) incorporated in FluoroMax™ particles (Seradyn Inc.). (Original publication III).

The up-converting phosphors (UCPs) were first introduced in the late 1990s (Wright et al. 1997; Zijlmans et al. 1999). They are composed of inorganic host lattices doped with lanthanides similar to the down-converting phosphors. However, only few lanthanide combinations, e.g. ytterbium with erbium/thulium/holmium, can exhibit up-conversion to visible light region upon non-coincident absorption of two or three infrared (IR) photons (Auzel 2002), a phenomenon unnatural among biological materials. The electronic transitions occurring during up-conversion and spectral features of up-conversion and down-conversion are illustrated in Figures 5 and 6, respectively. The ability of a material to up-convert is attributed to the long excitation lifetimes of the specific lanthanides, which, in turn, renders them susceptible to a second (or third) successive excitation event before the transition to the ground state. This leads to valence electrons of the emissive ion excited to a higher emission energy level, which is proportional to the number of excitation events during the excited metastable state (Soukka et al. 2005). The emission peaks of UCPs are, characteristic of lanthanide emission, sharp and well-defined. The IR excitation light (980 nm), emitted by e.g. a laser diode, has practical assets, because IR wavelengths traverse biological materials effectively. Hence, assays relying on UCPs are completely autofluorescence-free. This is contrary to UV-light, mainly used to excite down-converting lanthanide complexes, which causes autofluorescence and can be deleterious for both the biological materials and organic chelates of the down-converting luminophores. Consequently, careful selection of optical components in the up-conversion detection system is not required (Soukka et al. 2005). Also, in assays utilizing UCPs, the external environment does not affect the optical properties, thus a variety of materials are suitable as sample matrices (Niedbala et al. 2001). However, the non-functional surface of sole UCPs and the challenges of capping (Feng et al. 2003) impede the reproducibility of UCPs at present.
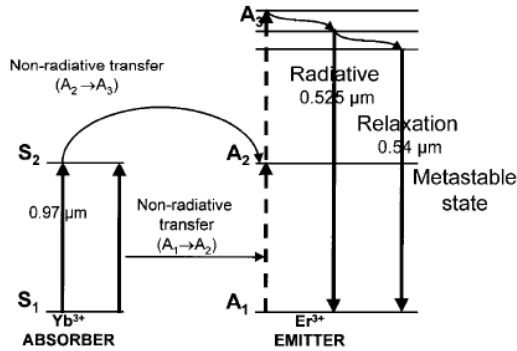
Figure 5. Up-conversion presented as electronic transitions. (Niedbala et al. 2001).
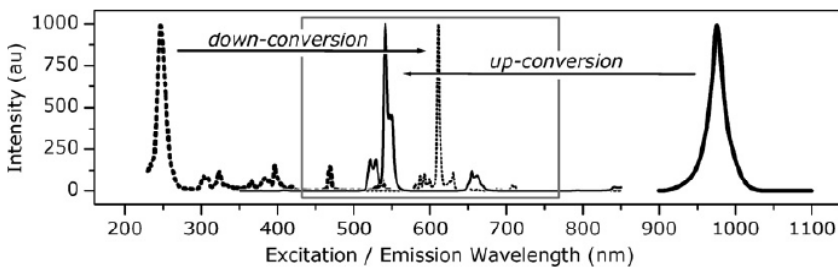
Figure 6. Down- and up-conversion translated into respective excitation and emission spectra. The down-conversion spectra represent that of the europium(III) ion-doped phosphor (Y_2O_3: Eu^{3+}). The up-conversion spectra represent the spectral characteristics of $NaYF_4$: Yb^{3+}, Er^{3+}. (Soukka et al. 2005).

The first experiments regarding the use of quantum dots, i.e. colloidal semiconductor crystals, took place in the 1980s with the aim of splitting water photocatalytically (Darwent & Porter 1981). Characteristic of semiconducting materials is that there is a gap between the valence and conduction band energy levels of less than 4 eV. The distinctions between conductors (such as metals), semiconductors and insulators are in the energetic state distinctions of valence and conduction band. The valence band represents all electronic ground energy states of an atom (at 0 K) and the conduction band the higher energy level(s) needed to move an electron or electron hole left in the valence band independently from one atom to another, thus creating conductivity. The excited electron and the hole may also be attracted by coulombic interaction forming an exciton. However, usually the exciton bears small binding energy and a large radius, and in crystals of nanometer size the exciton radius would be larger than that of the crystal. This leads to the most interesting property of the quantum dots, the quantum confinement effect (Brus 1983). It means that the radius of a crystal is close to or smaller than the exciton radius of the crystal lattice composition leading to discrete bandgaps between the valence and conduction bands proportional to the crystal size. This is explained by the increased kinetic energy required to fit the exciton in an extremely

small crystal. Essentially, this leads to an increasing bandgap when the crystal size is decreased, meaning that the smaller the quantum dot, the more excitation energy is required to excite valence electrons beyond the bandgap into the conduction band. The other way around, the excitation energy, e.g. photons, must only be higher than that of the emission wavelength characteristic of the quantum dot composition. The size of a quantum dot is between 2 and 10 nm in diameter. Beyond this size, the quantum confinement effect is lost, and fluorescence is not observed. When exploited effectively, the properties of quantum dots ensure a large and adjustable Stokes' shift. Compared to conventional small molecule luminophores, quantum dots are brighter and feature high quantum yields. Also, as quantum dots of different composition show emission spectra of distinct nuances (Bailey & Nie 2003), harnessing these characeristics could enable multiplexed assays as described by Han et al. (2001). Quantum dots resemble more the characteristics of a conventional fluorophore or a fluorescent protein that can be coupled to a large biomolecule. Given that a quantum dot surface can be activated with a multitude of reactive moieties, a single crystal of 5 nm in diameter may act as a solid support for two to five molecules according to Chan & Nie (1998). With the small size resulting in rapid kinetics and in vivo-compatibility (Zimmer et al. 2006), the premise of this label type is great. However, the limitation of quantum dots is the size-dependent emission character resulting in a restricted ability to tailor the spectral properties irrespective of the size. Also, they are challenging to fabricate and purify and they exhibit fluorescence intermittency (Nirmal et al. 1996).

The extraordinary features of colloidal gold were first discovered by Faraday (1857), who experimented the color-colloid size relationship in suspensions. Since then, gold particles have been used as probes in electron microscopy (Hayatt 1989), followed by the utilization as metallic catalysts (Schmid 1992) and as building blocks for nanoscale devices (Clarke et al. 1998). They have also been viewed as interesting labels due to special electrochemical characteristics (Dequaire et al. 2000; Liu & Lin, 2005), size-dependent surface plasmon absorption, high quantum efficiency and high emission intensity (Link & El-Sayed 2000). Gold particles exhibit photoluminescence that is attributable to the radiative recombination of the excited electrons to electron holes in the half-occupied conduction band. When the photons are absorbed, the relaxation processes of the electrons and holes culminate into phonon scatterings, some of which recombine to produce luminescence. However, while the luminescent properties, including wavelength shifts and intensity alterations, are size-dependent, albeit not classified as quantum confinement effect, they are also susceptible to solvation and different surface characteristics of the particle including reactive groups (Wilcoxon et al. 1998) and morphology (Mooradian 1969; Boyd et al. 1986). Nevertheless, the interest regarding the exploitation of gold colloids in bioaffinity assays has been substantial. One of the explanation is the ease of preparation. They have been especially used in strip-based

(Verheijen et al. 1998; Putalun et al. 2004; Wang et al. 2007) and DNA-hybridization assays (Tomlinson et al. 1988; Taton et al. 2000). Probably the most notable commercial bioaffinity products involving gold colloids are the heterogeneous DNA-hybridization assays produced by Nanosphere Inc. (IL).

Different particle species described above are compiled in Figure 7, which elucidates the arbitrary size ranges.
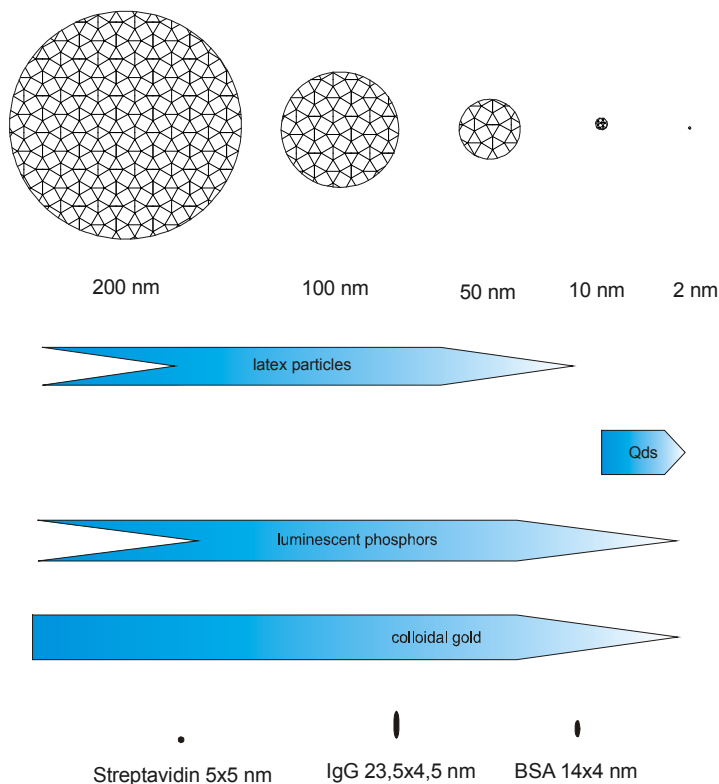
Figure 7. Dimensions of particle labels and common molecules utilized in bioaffinity assays. The actual dimensions of luminescent latex and phosphor particles extend to micrometer range. The dimensions of BSA and IgG are taken from Fair & Jamieson (1980). The dimensions presented are in proportion. Qds = quantum dots.

2.3   Particle fabrication

Polymeric latex and silica particles

Most commonly the compounds used in the preparation of polymeric particles are styrene or silane derivatives. Although many techniques have been introduced in literature, the principle polymerization methods for styrene and silane were described by van den Hul & Vanderhoff (1970) and Stöber et al. (1968), respectively. Empirical descriptions of the methods are given here. In the polymerization of styrene, the reaction involves

styrene monomers which will constitute the structure, the surfactant which surrounds the hydrophobic monomers, and an initiator which triggers the polymerization reaction. In the preparation of silica particles, the silane derivatives used in the condensation reaction dictate the surface characteristics. Similarly, the polymerization of styrene usually employs selected copolymers, which introduce critical or exploitable moieties onto the particle surface (Lück et al. 1998). Since styrene is a hydrophobic molecule, charged monomers, e.g. acrylic acid can be added as copolymers to provide hydrophilicity and thus monodispersity to the particles in water. Also, the carboxylic groups of these acids provide an opportunity to subsequent modifications of the particle surface, which is a crucial property of a particle. In addition to carboxylic groups, other copolymers introducing amine-, amide-, sulphonate-, hydroxyl-, aldehyde-, epoxy-groups and poly(ethylene glycol) (Gessner et al. 2002; Hou et al. 2007; Matsuya et al. 2003) have been utilized to obtain a desired surface character. Equally, various silane derivatives bearing functional chemical groups can be used to achieve different surface properties (Bagwe et al. 2006). The modification of the surfaces is important in functionalizing of the particles with biomolecules or for the eventual assay performance involving the aspects of folding of binding molecules coupled onto the surface (discussed below) and non-specific binding. Therefore, a careful selection of particle surface chemistry is important whenever a particle-based assay is optimized.

The size of the polystyrene particles is mainly controlled by the stoichiometry of the starting materials, especially by the amount of the surfactant, and by the conditions for seed formation as described by Shim et al. (1999) and André & Henry (1998). The stoichiometric approach also applies to the preparation of differently sized silica particles, despite the variety of techniques proposed (Kortesuo et al. 2001; Masuda et al. 1990; Isobe & Kaneko 1999; Vogel et al. 2007).

Polystyrene particles are usually doped with fluorophores after the polymerization is complete. However, the embedding may also take place during the polymerization as shown by Chen et al. (1999) and Tamaki & Shimomura (2002). The more conventional procedure of dyeing polystyrene particles relies on the hydrophobic properties of the fluorophores to be incorporated as described by Huhtinen et al. (2005). As the particle core is hydrophobic and the particle shell and external conditions mostly hydrophilic, the fluorophores are preferably localized into the core. On the other hand, fluorescent silica particles have been prepared with the fluorophore incorporated in the condensation reaction (Sokolov et al. 2007; Santra et al. 2001; Ye et al. 2004) or the fluorophore covalently attached to the silane monomer prior to polymerization (Hai et al. 2004). The latter is an effective alternative to circumvent the dye leaking issue, which is possible especially in the case of non-covalently doped polystyrene particles. The polymerization and dyeing are followed by a purification step, wherein the excess of fluorophores are removed (Frank and Sundberg 1981a, 1981b) by size-exclusion.

Inorganic lanthanide crystals

Inorganic downconverting lanthanide phosphors are lanthanide(III)-doped crystals produced using e.g. lanthanide(III) salts, oxides, sulphides, vanadates, alumina, strontium chloroapatite or phosphates (Meyer et al. 2003; Feng et al. 2003; Stouwdam et al. 2003; Beverloo et al. 1990; Wakefield et al. 1999). The predominant ions used in the lanthanide crystals are europium(III) and terbium(III) due to their longer fluorescence lifetime. The fluorescence of sole lanthanide(III) ions is weak. This stems from the parity forbidden 4f-4f intra transitions of the lanthanide ions (Laporte & Meggers 1925). The surrounding crystal fields render the 'Laporte rule' more forgiving to the extent that luminescence can be observed (Wakefield et al. 1999). Therefore, many crystal lattices doped with lanthanides may be luminescent and useful as label particles. In the specific lattices such as $LaPO_4$ doped with europium(III), the europium ion is coordinated with oxygen, which absorbs and transfers the excitation energy to the lanthanide (Stouwdam et al. 2003). In a vanadate-based lattice $LaVO_4$, different lanthanides can be utilized to form fluorescent particles (Stouwdam et al. 2005). Lanthanide crystals may be prepared first as bulk material of moderately high grain size, e.g. 1-10 µm in diameter, and then ground to smaller units of submicron size. (Beverloo et al. 1990, 1992). This tends to result in a heterogeneous particle population, i.e. a mixture of particles with various shapes and sizes. In addition, mechanical grinding introduces imperfections to the crystal structures, which may inflict luminescence attenuation (Berverloo et al. 1990). In this regard, a more desirable approach is to synthesize small crystals using a bottom-up strategy rather than the top-down approach. This may be conducted by using lanthanide(III) salts in conjunction with a carefully adjusted metal complexing chemistries (Bazzi et al. 2004; Stouwdam & van Veggel, 2004), wherein the crystal size may be controlled by adjusting the stoichiometry of the precursors. Similar control over the crystal size is featured in a combustion technique, in which the phosphors are formed by the evaporation and combustion of rare-earth nitrates, e.g. yttrium nitrate and lanthanide nitrate together with glycine as the fuel (Ye et al. 1997; Sun et al. 2000). The subsequent capping of the formed crystals is critical either due to the hydrophobicity (Feng et al. 2003) or the inertness of the surface to the subsequent biomolecule attachment. Most importantly, the quantum yield of the crystal may be significantly improved if an undoped layer is assembled as a shielding element (Kömpe et al. 2003). This is explained by the energy transfer processes to the surface through adjacent dopant ions or because the luminescence of the dopant ions at the surface is quenched (Huignard et al. 2000). Crystals of higher quantum yields may be synthesized as core-shell particles as explained by Kömpe et al. (2003). In order to provide a surface with functionality, crystals may be prepared in the presence of e.g. polyacrylic acids (Feng et al. 2003; Beverloo et al. 1990; Beverloo et al. 1992) or polyols (Bazzi et al. 2004), which provide negative charge onto the surface. Due to these surface moieties, the monodispersity of the crystals in suspensions is promoted and the particles can be subjected to either passive or active coupling of biomolecules.

The structure of UCPs is similar to the down-converting crystals in that they are composed of inorganic host materials doped with selected trivalent lanthanides. A common UCP lattice is composed of yttriumoxysulphide doped with absorbing ytterbium ions and emitting erbium ions (Zijlmans et al. 1999) (see also Figure 5.). Thulium(III) and holmium(III) have also been employed as dopants, and other host lattice materials, oxyhalides, fluorides, gallates and silicates are utilizable (Ziljmans et al. 1999). The emission wavelength is also dictated by the lattice material (Zarling et al. 1997). The UCPs of appropriate size for bioaffinity assays may be prepared from bulk material by grinding (Soukka et al. 2005) or by using a precipitation method (Sordetelet & Akinc 1988; Rossi et al. 1997; Corstjens et al. 2005). Another approach is the combustion technique also used to prepare down-converting phosphors (Tessari et al. 1999; Pires et al. 2005), wherein a very small crystal size is achievable.

Quantum dots

The most broadly applied quantum dots are composed of CdS and CdSe, i.e. of a combination of II-VI elements. Also other sulphides and selenides in addition to oxides, halides and tellurides have been reported (Henglein 1988; Brus 1991; Wang & Herron 1991; Murray et al. 1993). In addition, combinations of III-V elements, (InP and InAs) have been utilized (Olshavsky et al. 1990; Ushida et al. 1991; Pötschke et al. 2004). Two synthetic routes are widely employed. Aquous synthesis may be conducted using precipitation of e.g. H_2S or H_2Se or their metal salts from a solution containing the metal ion, using AsH_3 or $As(CH_3)$ when preparing arsenides or by the hydrolysis of alkoxy compounds when preparing oxides (Weller 1993). Alternatively, the preparation may be carried out employing an organometallic synthesis as described by Murray et al. (1993) wherein an organometal such as dimethyl cadmium is mixed with a coordinating solvent, e.g. tri-n-octylphosphine. The growth mechanism of quantum dots during the precipitation reaction follows Ostwald ripening. According to this theory, the smaller particles dissolve and the monomers released thereby are consumed by the large particles which are less susceptible to dissolution. Hence, quantum dots of larger size are produced as the reaction is prolonged, and therefore, precipitants collected from the reaction at designated time points (Murray et al. 2000) correspond a distinct quantum dot size. The surface of the quantum dots is modified with stabilizers such as sodium polyphosphates or thiols in order to regulate the growth rate and the size of the particles during synthesis (Weller 1993) and to preserve the crystal structure from photochemical decomposition (Dabbousi et al. 1997). This is critical for quantum dots due to the small particle size and a consequent high surface-to-volume ratio. Without the passivation shell, the photocorrosion upon excitation would be significantly higher due to the decomposition of the emittive crystal material itself via radical formation or attack by oxygen (Spanhel et al. 1987). Given the effect of quantum confinement, the size of the quantum dots of specific composition is of critical importance due to the size-related split of energy bands, i.e. spectral characteristics. In addition to

temporally collected precipitates, the size of the crystals can also be controlled altering the concentrations of the precipitants or stabilizers, or subjecting the seed formation to different conditions (Weller 1993). A quantum dot preparation with high size deviation would result into a multitude of emission bands rendering the overall emission spectrum broad with low intensity. Therefore, besides the temporal separation of formed precipitates, a careful purification scheme, e.g. size-exclusion chromatography and gel electroforesis in tandem, must be conducted in order to obtain a homogeneous population of quantum dots in a given preparation (Eychmüller et al. 1990). This aspect is also emphasized by the complexity of the chemical reactions employed in the preparation, and thus, by the minimal variations at different stages of synthesis leading to large batch-to-batch deviations (Weller 1993).

Gold particles

Colloidal gold is produced by co-ordinating gold atoms into molecular networks. Currently, stable gold particle suspensions can be prepared in 1-250 nm particle diameter range. While metallic particles in general can be prepared using e.g. radiolysis, thermolysis, photolysis or electrolysis of metal containing precursors, the oldest and most widely used technique for preparing gold particles employs the reduction of the metal salt in solution (Link & El-Sayed 2000). Particles of size 10-20 nm in diameter have been produced by the reduction of tetrachloroauric acid (or chloroauric acid) with sodium citrate in boiling conditions (Frens 1973; Horisberger 1979). First, the citric acid acts as a reducing agent, later it is adsorbed onto the formed clusters to introduce negative charge onto the particles. By controlling the concentration of the reducing agent the particle size can be adjusted; the less citric acid is present, the larger particles are produced due to charge depletion and consequent aggregation. To produce smaller particles, the method of Brust et al. (1994) has been employed. Briefly, tetrachloroauric acid is mixed with tetraoctylammonium bromide in toluene, and the cluster formation is initiated by the addition of a reducing agent. The number of gold atoms per particle is directly proportional to the size of the cluster as described by De Roe et al. (1987). Numbers of nuclearities are 13, 55, 147, 309, 561, 923 and 1415, with the arrangement in closely packed 1-7 coordination shells (Rapino & Zerbetto 2007). Different shapes of colloidal gold, i.e. spheres, rods or pyramidal structures result in distinctions in regard to electrochemical characteristics (Aubin-Tam & Hamad-Schifferli, 2008). The surface of the formed clusters is relatively inert, although it may react with thiols, and to a lesser extent with primary amines and carboxyl groups. Therefore, a capping procedure is often conducted if a covalent coupling of molecules onto the surface is desired. For instance, alkanethiols form a protective layer onto the clusters (Verma & Rotello 2005) and can be introduced onto the surface already at the stage of cluster formation. The monolayers of capping ligands can then be exchanged with other functional groups resulting in mixed monolayers of diverse functionalities (Templeton et al. 1998). However, a wide range of other functional ligands may also be introduced already at the cluster formation stage

(Verma & Rotello 2005). As stated, the preparation of gold colloids is relatively easy to conduct facilitating their applicability.

2.4   Particle functionalisation

Passive physical adsorption

The surface character of the particles defines the conjugation chemistry by which a desired coating is achieved. In the simplest scenario, passive adsorption is employed. This usually involves protein molecules capable of interacting with surfaces through hydrophobic and electrostatic interactions or hydrogen bonding. The characteristics stem from different amino acid configurations and molecule conformations (Gessner et al. 2002). Although the surface moieties introduced onto the particle surfaces during the polymerization of latex or precipitation of inorganic colloids (including e.g. carboxyls, amines, sulfonates) do not function in a specific manner in the case of passive adsorption, they do partly dictate the adsorption efficiency of the molecules (Lück et al. 1998; Gessner et al. 2002). Other parameters affecting the adsorption efficiency are the external conditions, mainly pH-value and ionic strength, and the nature of the molecule to be bound, its exposing amino acid side chains and structural tendency to conform to adsorption (Yoon et al. 1996; Elgersma et al. 1992; Shirahama & Suzawa 1985; Li et al. 2005; Shirahama et al. 1989). The effect of pH-value being close to the pI-value of the protein does not only translate into more efficient adsorption, it may also promote the activity of the adsorbate as described by Kondo et al. (1993). An overall consensus on the roles of different interaction types, i.e. hydrophobic and electrostatic interactions and hydrogen bonding, in protein adsorption has never been met (Hou et al. 2007), and in reality, the event may be a mix of all non-covalent interaction types affecting each other (Yoon et al. 1999) irrespective of the protein or the particle surface to be conjugated. In-depth reports on protein adsorption onto differently modified lattices are available (Elgersma et al. 1990, 1992; Suzawa et al. 1982; Shirahama et al. 1989; Shirahama & Suzawa 1985; Li et al. 2005; Liu et al. 2006; Okubo et al. 1990). The literature helps to understand the complexity of adsorption and the relevancy of the phenomenon in the functionalization of particulate labels, even despite the primary coupling method selected.

Active coupling

Since adsorption may not produce the most active surface due to the probability of adsorbate conformational change (Welzel 2002; Verma & Rotello 2005; Bower et al. 1999), an aspect, which also has controversial opinions (Aubin-Tam & Hamad-Schifferli 2005; Brown et al. 1996; Zhao et al. 1996), more specific coupling schemes are generally favoured. This may also be explained by the less persistent nature of adsorption due to the reversibly and irreversibly bound molecules. Moreover, covalent coupling is often considered a necessity for small molecules to be coupled due to e.g. a poor adsorption tendency or emphasis

in specific orientation. A large number of covalent coupling technologies exists and only few examples are given here. These include the conjugation through linking molecules introduced on the particle surface, indirect linkage via specific affinity of e.g. a protein for a cofactor, here designated as bioreactive coupling, and direct covalent attachment onto the particle surface moieties. These interaction types are presented in Figure 8.

Linking molecules

Bioreactive coupling

Direct conjugation
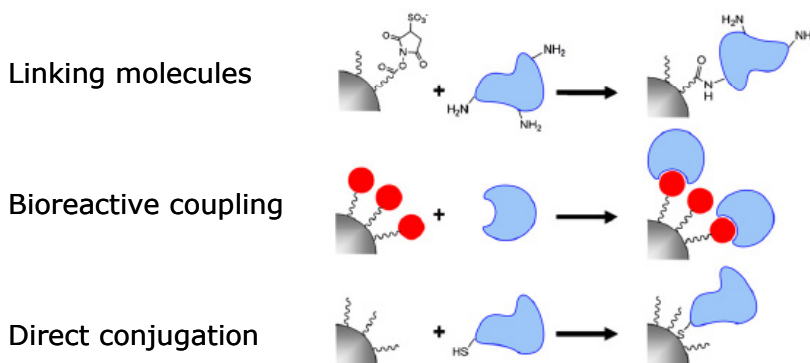
Figure 8. Specific strategies of molecule attachment onto the particle surfaces. Taken from the report of Aubin-Tam & Hamad-Schifferli (2008).

The coupling of molecules onto the particle surface via chemical linker molecules is a popular means to surface functionalization. This does not only yield more control over the stoichiometry of the coupling density compared to adsorption, it may also provide the ability to modulate the distribution of coupled molecules (Hainfeld et al. 2000), or the morphology of the surface ligands (Jackson et al. 2004). In the book by Hermanson (1996) the linking of e.g. carboxyl groups and molecules bearing primary amines by using EDC (1-ethyl-3-(3-dimethylaminopropyl) carbodiimide hydrochloride) and NHS (N-hydroxysuccinimide) as coupling agents is explained. The chemistry is widely applied to biomolecular coupling, and it was also utilized in the original publications I-IV. However, usually the reason for not introducing such chemical moieties onto the particle surface already at the stage of particle preparation (capping or copolymerization) lies behind the susceptibility of these reactive groups to inactivation by e.g. hydrolyzation. Therefore, the attachment of the linking molecule and the subsequent reaction with the molecule to be coupled is usually carried out rapidly within hours, unless such linkers are introduced onto the surface during the polymerization as protected molecules (Ganapathiappan & Zhou 2006). For an overview of different coupling chemistries involved in protein immobilization and modification through different amino acids, see the review of Brinkley (1992). Another possibility to coupling is to introduce metal-chelating groups, such as NTA (nitrilotriacetic acid), onto the particle surface to interact with histidine-tags of e.g. recombinant proteins (Abad et al. 2005; Kim et al. 2007). The most important trait of the linking molecules is that they are highly reactive resulting in efficient coupling.

Bioreactive coupling may be a feasible alternative for conjugating molecules onto the surfaces, especially in the development of heterogeneous assays. In this method, the high affinity binding interaction between two biomolecules is utilized to attach the desired molecule onto the particle surface. The coupling is preceded by the immobilization of the other biomolecule partner onto the particle surface, which may be achieved by passive physical adsorption or a covalent coupling chemistry. A classic example of bioreactive coupling is the biotin-streptavidin system, which can be classified as nearly covalent by its affinity (dissociation constant Kd-value of 1×10^{-14} M) (Green 1990). This interaction is exploitable as a coupling method, e.g. when the biotin is conjugated to a molecule of choice and the particle surface is derivatized with streptavidin molecules. However, despite the extremely high natural affinity and the benefit of the quadruple valence of streptavidin practically rendering the orientation of the molecule a non-factor, the efficiency of the coupling is eventually defined by the interface created by the biotin- and streptavidin-partners as suggested by Swift & Cramb (2008). The same disadvantage hampers other bioreactive coupling systems such as the antibody-antigen system (Ackerson et al. 2006) along the fact that antibodies as larger molecules and only divalent in nature, as in the case of IgG, can assume multiple orientations despite the coupling chemistry. This affects the overall activity of the surface-bound fraction. However, this approach is widely utilized due to its specificity and affinity, even though the affinity value (Kd > 1×10^{-10} M) does not compete with that of the streptavidin-biotin system. The research around aptamers (Ellington & Szostak 1990) may also contribute to the variations available in the bioreactive coupling scheme. The idea behind aptamers is theoretically sound as these molecules can be designed according to their binding counterparts and prepared with simple nucleic acid/ peptide chemistry. Despite the specificity of bioreactive coupling, principally it may not be feasible in applications which rely on the proximity of the interacting species, i.e. the space between the particle and the molecule binding onto its surface-conjugated counterpart as e.g. in FRET, because of the size of the molecular complex in bioreactive coupling is usually larger than required for efficient energy transfer (Stryer 1978; Selvin 1995). However, as shown in original publication III, the distance may not be of as critical importance as imagined in the case of particulate labels acting as both donors and acceptors.

Contrary to the bioreactive coupling, the direct coupling of binding molecules to surface reactive groups, introduced already at the polymerization or capping stage, is more suitable for e.g. the aforementioned FRET applications. This ensures that the distance between the conjugated biomolecule and the particle luminophores is minimal. These moieties should be more tolerant to environmental effects than are the linking molecules presented earlier, and they may be readily reactive for binding with e.g. amino acid side chains of the proteins. For instance, aldehyde groups on a polystyrene particle react with protein amine-groups (Rundström et al. 2007), gold colloids react with thiol-groups (Ullman 1996) as do sulphur containing quantum dot shells (McMillan et al. 2002). However, one of the

concerns regarding the use of direct conjugation is the potential of steric interference, which is related to the bulk of the particle and the molecules brought at extremely close proximity. This could culminate into prohibition of the specific conjugation reaction as well as adsorption (Aubin-Tam & Hamad-Schifferli 2008).

The most desired way of binding molecules onto particle surfaces would be through site-specific attachment. Ideally, this means the coupled protein would protrude from the surface in a manner that enables the most efficient activity minimizing the effect of random orientation and the consequent blockade of binding sites (Fig. 9). This could be accomplished by e.g. a site-specific biotin modification to an antibody in conjunction with a streptavidin derivatized surface as described by Ylikotila et al. (2006). However, site-specific coupling is strongly reliant on the composition of the molecule to be coupled. For instance, a unique amino acid exploitable in site-specific conjugation is not a typical trait of a large protein, as the number of different amino acids is limited to only 20. As a resort, the protein structure can be modified so that a new amino acid, most commonly containing an amine- or thiol-group, is properly exposed on the protein surface (Ylikotila et al. 2006; Aubin et al. 2005; Brennan et al. 2006). Also, specifically attached His-tags may be used as anchors (Abad et al. 2005; Hu et al. 2007; Hainfeld et al. 1999) if Ni- or Co-NTA derivatized particles are employed. Alternatively, the molecule can be modified void of other reactive groups leaving a specific chemical group available to conjugation as suggested by Yamamoto (2003) and Konterman (2005), given that the molecule structure-function relationship does not change upon the modification. Ultimately though, despite how the site-specific coupling is executed, the immobilization of molecules in an ideal orientation gains a lot of attention in the many scientific fields involving surface chemistry.
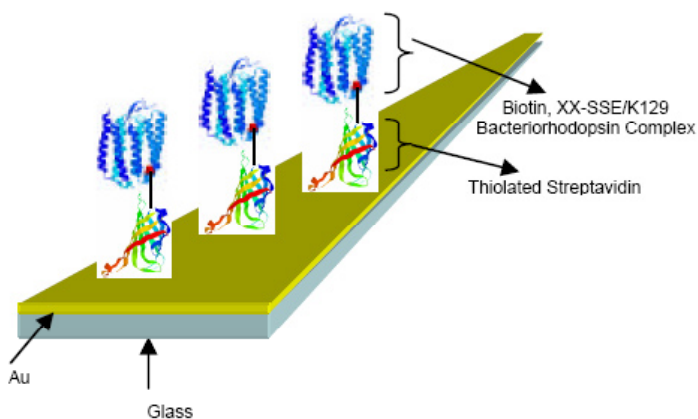
Figure 9. Site-specifically labeled molecules can be conjugated onto surfaces with correct binding orientation. In this example, both the streptavidin and bacteriorhodopsin complex have been modified to create a homogeneous surface (Ho et al. 2003).

Regardless of the selected coupling method, a significant fraction of molecules, especially proteins, bound onto the particle surface are passively adsorbed. The propability of this occurrence becomes more pronounced as the molecule number-to-particle surface area ratio in the conjugation is increased. Even though this may be viewed as a drawback in terms of the stability of e.g. protein coating, it may also promote colloidal stability of the particle suspension, if the reactive groups of the particles introduce a charge onto the surface in addition to the potential to covalent conjugation, and the charge is not depleted upon the covalent conjugation. Surface charge on colloids is highly recommended due to enhanced monodispersity, which is bound to promote reproducibility of an assay. Hence, the strategy of the active coupling should be tailored to also support adsorption to ensure as efficient protein coverage as possible. Therefore, fine-tuning the reaction conditions is a balance between the ideal pH-value for the reactive groups involved in the specific coupling reaction and the ideal pH-value for the molecule to be coupled. In the case of protein coupling, this is explained by the protein conformation being the most active (Kondo et al. 1993), stable and the adsorption being most efficient at its isoelectric point pI. Also, adjusting the ionic strength is important in a passive adsorption susceptible to pH-value deviations (Shirahama et al. 1989). On the other hand, the choice of the chemical moiety on the particles surface used for covalent coupling or to promote monodispersity can greatly affect the activity of the adsorbate. This has been confirmed in the studies of Aubin-Tam & Hamad-Schifferli (2008), who conducted circular dichroism evaluations for a protein adsorbed on differently derivatized surfaces.

Commonly, inorganic lanthanide phosphors, both down- and up-converting, in addition to quantum dots, are prepared with no initial surface functionality. Thereby, the coating of binding molecules must be preceded by a surface activation phase if a covalent coupling is to be achieved. Alternatively, the phosphors may also be coupled with binders via physical adsorption onto the capping layer (Beverloo et al. 1992). A common resort to introduce chemical moieties onto the surface is to polymerize a thin layer of silica (Ohmori & Matijevic 1992), and to select e.g. an amine- or sulfhydryl-modified silane derivative. However, as stated earlier, the additional modification step makes the coating of inorganic phosphors more labor-intensive. Also, the modification requires careful optimization in order to obtain homogeneous particles with minimal batch-to-batch variation (Feng et al. 2003). The thickness of the reactive shell layer may also be highly important, if the modified surfaces are applied to assays requiring a close proximity of the particle surface and the surface-bound biomolecules upon assay reaction (e.g. in FRET-based assays).

The characterization of particle coating

The method of characerizing the molecule coating depends partly on the particle size. For small particles, e.g. 2-10 nm in diameter, one can apply techniques to probe the actual structure of the adsorbed molecules. Such techniques include direct imaging

using electron microscopy (Hu et al. 2007), circular dichroism (Vertegel et al. 2004; Lundqvist et al. 2006; Narayanan et al. 2007; Mamedova et al. 2001), optical spectroscopy if the coated molecule bears a chromophore or an absorptive moiety (Aubin-Tam & Hamad-Schifferli 2005) and x-ray scatterings (Srivastava et al. 2005). Another approach is the functional analyses, which assess the actual activity of the bound molecules. This is also applicable in the evaluation of larger particles, on which the extent of attached molecules is usually increased by a significant margin rendering the evaluation of protein structure per se more difficult to interpret. Therefore, one can apply more arbitrary approach for assaying the activity of the coatings, which may give only a mean estimation regarding the activity of the surface. For instance, an antibody coating may be evaluated on account of binding site number using a labelled antigen (original publication III, Kokko et al. 2004; Soukka et al. 2001a, 2001b, 2003), or a streptavidin coating may be assessed with a labelled biotin (Kokko et al. 2007, original publication IV). Using this method, the number of binding sites, i.e. the average number of sites per one particle in the given preparation can be calculated. However, this figure does not reveal the proportion of denatured or disoriented molecules on the particle surface. Despite this inability, rough approximations and comparisons between different particles bearing different surfaces or comparisons between distinct preparation batches can be made.

Particle size influence on coating

It has been reported by Vertegel et al. (2004) that particle size may have a strong influence on how the molecules adsorb onto the particle surface during conjugation. However, this attribute is also dependent on the molecule to be attached because of the different interaction types affecting the coupling and the variety of compositions of different molecules. The conclusion of Vertegel and colleagues was that the potential of electrostatic interaction, viewed as the most dominant coupling force in the study, is proportional to the particle size. Hence, the size affects the type and the extent of prevailing non-covalent interaction types between the molecule and the particle surface. Furthermore, the curvature of a particle may also dictate the conformation of the molecule to be attached as elucidated in Figure 10. This is explained by the "number" of interactions between the molecule and the particle being proportional to the particle size. Essentially, because the curvature of a larger particle is less steep, it promotes an increased surface-to-surface interface area per interaction. Based on this observation, it is suggested that the protein retains its native conformation better when adsorbed onto smaller particles. On the other hand, the results of De Roe et al. (1987) suggest that the dissociation of molecules adsorbed onto the particle surface is inversely proportional to the particle size. The authors were not able to verify the reason for the behaviour, although one might assume the "number" of interactions being small at the molecule-particle interface is at play here as well.

However, given that the aforementioned studies involved different particle types and different proteins, one cannot compare the results directly because of the completely different molecular interfaces. Eventually though, the nature of the molecule, i.e. the tendency to conformation changes upon association, which is defined by the rigidity of the molecule and only influenced by the particle surface, dictates its activity and persistency on the particle. Additionally, given the finite size distribution of particle preparations in general, a simple conclusion regarding the protein conformation and its consequences cannot be drawn.
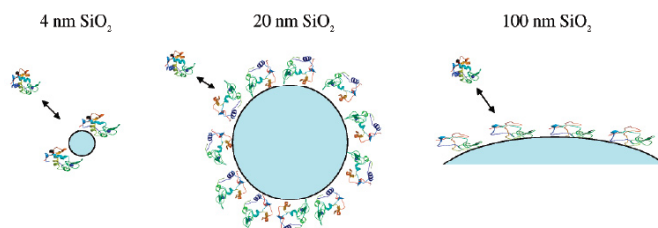
Figure 10. The impact of particle size on the adsorption of lysozyme onto silica particles as suggested by Vertegel et al. (2004).

As a practical aspect, the removal of unbound molecules after the coupling reaction becomes more challenging to execute with decreasing particle size. This is explained by the difficulty to use size exclusion when the particle size is close to the molecule size. For larger particles of 150 nm in diameter and beyond, it is convenient to use a simple centrifugal sedimentation technique. The smaller particles (2-100 nm in diameter) must be purified using filter devices or more labor-intensive chromatographic methods. This leads to a more complex purification scheme, which is also prone to increased variation regarding the particle yield and functional properties. Gold colloids are exceptional in this regard due to their higher density; even particles of 50 nm in diameter or less can be sedimented with a conventional centrifuge.

Practical considerations – do we throw tactics out of the window in the end?

In reality, the theoretical predictions may not produce the best performing coating for an assay because of the potential adverse effect of a dense molecule coverage. This may be observed as an increase of non-specific binding of the particle conjugates impairing the assay performance. The issues may be a product of depleted surface charge due to the dense coating, the hydrophobic character of the coated molecule, or the size-hydrophobicity combination of the particle conjugate poorly promoting monodispersity according to thermodynamics. Also the potential increase of agglomeration of the particles induced by e.g. a dense protein coverage may decrease the shelf-life of the preparation. Further, a dense coverage may lead to protein crowding, increased denaturation of the adsorbed proteins and steric issues such as prohibiting the desired

binding reactions in an assay (Aubin-Tam & Hamad-Schifferli 2008). This however, seems to be an inherent property of the protein in question as suggested by Vertegel and colleagues (2004). In homogeneous assays, e.g. where particulate labels are employed as FRET donors, a highly dense molecule coverage may inflict self-quenching of conventional acceptor fluorophores binding onto the surface due to the close proximity and intermolecular fluorescence attenuation (Kokko et al. 2004, original publication IV).

Given that the outcome of a coating is reliant on a multitude of aspects, often a trial-and-error-type approach seems a feasible option. However, the knowledge of theoretical background facilitates the designing of the experimental scheme. Essentially, aspects worth consideration are the type of binding molecule to be bound (pI-value, hydrophobicity, tendency to adsorption through conformational flexibility), other known assay components (buffer and reaction chamber composition, analyte properties, other binders in the system and matrix effects inherent to the samples to be used), the size of the particle and the type of surface (functional groups and backbone material) it possesses.

2.5   Particle size influence in bioaffinity assays

Common features

The most important size-related aspect in an assay is the binding kinetics (Härmä et al. 1999). This is accompanied by the density and activity of the coating of the particles (Swift & Cramb 2008) as well as the dose of the analyte. The diffusivity of a particle conjugate is proportional to the radius of the particle defined with Einstein-Stokes equation $D = kT/6(pi)r\mu$, where D is the Brownian Diffusivity, k is the Boltzmann's constant, T is temperature, r is radius and μ is the viscosity of the medium. On the other hand, the monovalent affinity of a binding molecule is, at least to the point of crowding-related issues, proportional to the density on the particle surface (Soukka et al. 2001a). According to diffusion rate, the smaller the particle size, the more rapidly the binding will occur on average. This is especially the case if similar particulate surfaces, i.e. equal total surface area and equal parking areas of functional groups and binding molecules, are subjected to reaction. In this regard, a small particle size is preferred because a shorter turnaround time is achievable due to this kinetic advantage. On the other hand, the experiments of Swift and Cramb (2008) indicate that the size of the interacting species in an assay is not a definitive answer to the assay kinetics, but also the surface tension effects of the interacting surfaces, i.e. coated nanoparticles and other solid phases (other particle species or the surface of a reaction chamber), have impact. This was observed as ill-fitting particle size relationship to the kinetics measured. Even though these figures were determined using a separation-free method, the same effects apply in heterogeneous

assays. An asset of a small particle in the size range of 2-100 nm in diameter is the lack of sedimentation (except for the gold particles of higher density) during an incubation period where shaking or rotary motion is not applicable. Particles with the size beyond 200 nm in diameter sediment if not disturbed by a continuous motion. However from another practical standpoint, coated particles of 100 nm in diameter and beyond tend to maintain the monodispersity better because of the thermodynamic limitations (Taboada-Serrano et al. 2005).

To obtain the benefit of the improved monovalent affinity of a binding molecule associated with particulate labels, the larger particles are preferred due to the higher number of molecules attachable on the surface of one unit. Although not verifying the effect of particle size per se, Soukka and colleagues (2001a) determined the impact of binding site number to this affinity improvement using particles of 107 nm in diameter. On the other hand, quantum dots and small gold colloids act virtually as small molecule labels that are able to co-ordinate a few binding molecules onto the surface (Chan & Nie 1998). Due to the steep curvature of these particles, multiple concomitant interactions with a target molecule are limited, if at all possible.

Another aspect while selecting the particle size is the specific activity of the particle. As for most particles, this is also a size-dependent feature (Härmä et al. 2001). The high specific activity may be beneficial as well as impairing regarding to the assay performance (discussed below in more detail). However generally, it is a decision between slower kinetics, arguably better affinity, better colloidal stability and higher specific activity of a larger particle and the opposite properties of a smaller particle. Also, it is critical to take into account the interacting biomolecules, e.g. an antibody immobilized onto the particle and the antigen, since the larger the particle, the more probable is the steric interference on this interaction caused by the bulk of the particle.

Size impact on heterogeneous bioaffinity assays

At present, there are no profound reports regarding the particle size influence on the performance of heterogeneous assays. Therefore, a brief elaboration on the subject based on the geometries and kinetics of the particle–solid phase interaction should be carried out. In a particle label-based non-competitive two-site bioaffinity assay conducted in a conventional reaction chamber, e.g. in a microtiter plate well, the unbound or weakly bound label particles are separated from the ones specifically attached onto the well surface (Fig. 11). The depicted method is used as an example throughout this chapter. Prior to the second washing step (Fig. 11), the specific interaction of the particle conjugates and the analyte molecule bound onto the well surface had taken place. As stated above, the kinetics of this association is heavily reliant on the particle size mainly due to diffusivity but also due to the activity of the particle, and the nature and dose of the analyte. The size effect is even more pronounced in the case of a kinetic assay format

(original publication II), i.e. where the assay result is read prior to this binding reaction reaching equilibrium.

Non-specific binding is an issue which has significant impact on the assay sensitivity and reproducibility. It is a product of multiple aspects; the surface character of the particle and the well surface, which both involve the composition of surface materials and the properties of binding molecules (e.g. hydrophobicity), and matrix-related effects. Considering the immunofluorometric assay presented in Figure 11, it has been reported that the extent of non-specific binding is independent of the particle size and that the size has a significant effect on the specific signal favouring the use of small particles (Näreoja et al., unpublished data). Obviously, small particles react with higher probability to analyte molecules than large particles possessing slower kinetic properties.
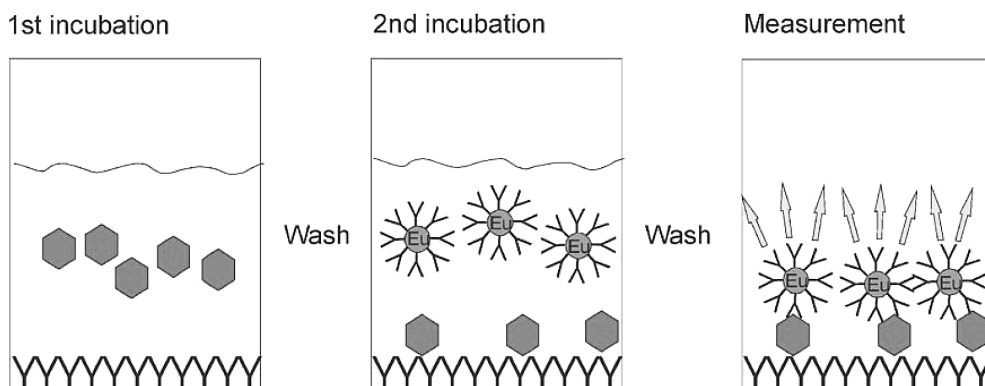
Figure 11. The principle of an exemplary nanoparticle-based heterogeneous non-competitive immunoassay. In the first incubation, the analyte is recognised by the antibodies immobilized on the solid phase of e.g. a microtiter plate well. The unbound material is washed away and the nanoparticles are introduced. Thereafter, a washing step is carried out and the fluorescence, proportional to the analyte dose, is detected using a fluorometer. (Original publication I).

Another size-related aspect, also projected in the results of Näreoja and colleagues, is the sterical effect a particle may exhibit as stated earlier. Comparing differently sized particles with equal surface properties, a smaller particle poses less sterical hindrance for the binding event due to the bulk of the particle being less obtrusive. This is only the case, if the sheer bulk of a particle label has a marked effect on the interaction, a phenomenon that is also reliant on the dimensions and orientation of interacting molecules at particle-well surface interface and the charateristics (e.g. charges) of the interacting surfaces. If this bulk factor exists, it contributes to the apparent slower kinetics in addition to the actual kinetics per se, because in this scenario, the average affinity of a binding molecule is lower on a larger particle. However, if the bulk of a particle does not cause a sterical issue in a practical particle size range, 50-200 nm in diameter, on average a

larger particle would provide a decreased dissociation rate because of the facilitated multiple simultaneous contacts. In an ideal case, where a multitude of binding molecules protrude perpendicular to the tangent of a perfect particle curvature, multiple concomitant interactions are allowed if a particle conjugate is sufficiently large and interacts with e.g. a solid phase covered with binding molecule-analyte complexes. This is especially the case if an analyte molecule is of size similar to the particle and contains multiple identical interaction sites as exemplified in the original publication I. The decreased dissociation of a larger particle would be explained by the curvature being less steep enabling a larger area of close proximity between the particle surface (the spherical cap) and the surface of the analyte. The effect would also be emphasized if a high dose of monovalent analyte was applied in conjunction with a high capture molecule density on the well surface enabling increasing number of simultaneous contacts with increasing spherical cap. For monovalent analytes of low analyte doses or low capture molecule density, the kinetic advantage of a smaller particle, especially the faster rotational velocity, compensates the aforementioned effect.

According to the most implicit theoretical approach, the ideal particle size in heterogeneous assays is determined on account of all the properties described. Hence, compromises between the aspects of kinetics, specific activity, steric hindrance and binding capacity must be made with many of the properties cancelling out each other. The most simplified interpretation of an ideal particle size in a heterogeneous assay is an imaginary limitation between a small particle, < 40 nm in diameter, being generally too small according to thermodynamics (Taboada-Serrano et al. 2005) causing extensive agglomeration irrespective of the particle material, and a large particle, > 150 nm in size causing slow kinetics (Härmä et al. 1999), potentially increased inactivation of the binding molecules (Vertegel et al. 2004) and being susceptible to gravitational force. Essentially, this renders the practical approach of selecting the particle size as a matter of trial-and-error. The most critical aspects regarding the selection of the particle size are compiled in Table 1. Extremely small particle labels like quantum dots cannot be considered in this sense, because of their size range maximum being approximately at 10 nm in diameter.

Table 1. Particle size dilemma – doped latex particles, silica particles and inorganic phosphors

Heterogenous assays	Advantage	Disadvantage
"Large particles" 50-200 nm in diameter	**Gentle curvature - potential of multiple concomitant binding events to multiepitope targets** **Better colloidal stability when functionalized**	**Slow kinetics** **Gentle curvature - increased protein denaturation** **Increased sedimentation** **Steric hindrance increased**
"Small particles" 2-50 nm in diameter	**Rapid kinetics - shorter assay turnaround** **No sedimentation** **Steep curvature - native protein structure maintained** **Steric hindrance decreased**	**Decreased colloidal stability when functionalized** **Steep curvature - less persistent protein adsorption**
Homogeneous assays (FRET-based)	Advantage	Disadvantage
"Large particles" 50-200 nm in diameter	-	High background fluorescence if donor fluorescence interference occurs
"Small particles" 2-50 nm in diameter	Less background fluorescence upon donor fluorescence interference	-

Aspects highlighted in **bold** are also valid in homogeneous assays

These predictions are established around the following characteristics:

i) fluorophore number per particle volume is equal

ii) surface character for each particle type is the same

Size impact on homogeneous bioaffinity assays

The effect of particle size on homogeneous assays is more complex than it is on heterogeneous assays. Even though the steric hindrance and the kinetics apply here as well, other factors can also have profound impact depending on the assay format. In FRET-based assays wherein the particles are employed as donors (see Table 1), the distribution of the emissive units, e.g. lanthanide complexes, within individual particles is important. In the preparation of latex particles, these complexes are commonly doped exploiting their hydrophobicity, and thus, the distribution inside the particles may be considered even. Therefore, due to the FRET range limitation (Stryer 1978; Selvin

1995) and the high specific activity of the particulate labels in general, this may become problematic if the emission spectra of the donor fluorophores overlap with that of the detection wavelength of the sensitized acceptor emission. The potential of this issue is best explained in Figure 12, wherein the fraction of donors participating in FRET is elucidated. In addition to latex particles, this problem is also prevalent with doped silica and inorganic lanthanide complexes, in which the lattice structure is composed of a homogeneous crystal, i.e. the whole particle exhibits luminescence. The interference of direct donor fluorescence is explained by the multitude of secondary emission peaks of lanthanides described earlier. Hence, the donor interference is proportional to the number of donor particles utilized, but it is also critically affected by the emission spectrum of the acceptor, and hence, the selected detection wavelength of the sensitized emission. To minimize the effect, it is advisable to adjust the amount of donors in an assay carefully, and to utilize a detection wavelength at which the direct donor emission is minimum and the acceptor emission maximum using a tailored emission bandpass filter.
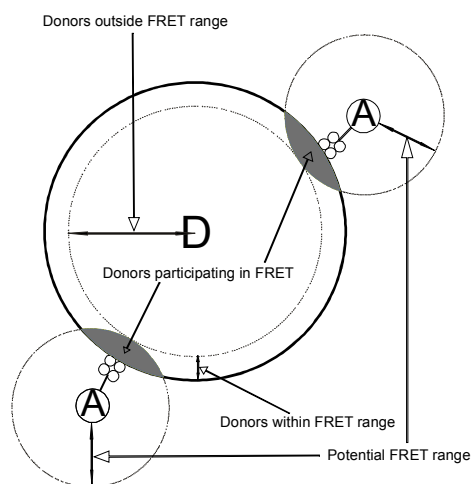
Figure 12. Potential of FRET-occurrence on the surface of particles doped with donor fluorophores. D = donor-doped particle; A = small molecule acceptor coupled to a protein. The dimensions are not in proportion. (Original publication V).

The particle size-related donor interference limiting the sensitivity of a FRET-based assay has also been highlighted by Meyer and colleagues (2003), who prepared inorganic core/shell lanthanide crystals to assign emissive properties only to the shell of the particle. In theory, this approach would be extremely feasible in terms of the colloidal stability of functionalized particles. This is explained by the ability to prepare larger particles without increasing the number of donor fluorophores excessively and by the larger particles forming less aggregates due to more favourable thermodynamics (Taboada-Serrano et al. 2005). More importantly, the cores void of lanthanide complexes would minimize the extent of interference related to direct donor fluorescence irrespective of the selected detection wavelength, if the shell thickness does not overly exceed the

FRET-range, the total of which is typically < 100 Å (10 nm). However, inspite of the theoretical background of direct donor fluorescence interference in FRET, the severity of the issue may not be as profound as presumed. This was highlighted in the original publication V, in which the donor interference of differently sized europium(III)-doped polystyrene particles was examined. The findings indicated the donor interference-donor size-correlation, but the interference was effectively overshadowed by the sensitized fluorescence, irrespective of the particle size. However, to optimize a FRET-based assay with rigour and with less requirements for the optical setup, the preparation of core/shell particles may be the way forward.

In other particle-based homogeneous assay technologies, SPA and LOCI (or AlphaScreen™), the particle size is not as significant, because the excitation energy emanates from the particle surface-bound isotopes or singlet oxygen, respectively. The principles of the detection techniques are fully reported in the publications by Hart & Greenwald (1979) and Ullman et al. (1996). In these technologies, no additional background fluorescence is produced with increased particle size irrespective of the luminophore distribution, because the emission of the donor is of different quantum species than that of the luminescent acceptor particles employed. Further, the excitation light in AlphaScreen technique is of lower energy level than the emission rendering the interference of excitation light insignificant. Overall, large particles are preferred in these techniques to increase the acceptor signal and to promote the colloidal stability. In agreement with this projection, the typical AlphaScreen kits (PerkinElmer Life and Analytical Sciences) are provided with particles of size 250 nm in diameter. The size of the SPA beads (GE Health Care Life Sciences) is even larger, generally 2-8 μm in diameter.

The extraordinary feature of quantum dots of specific chemical composition is their size-dependent excitation and emission properties. Since the overall luminescence production mechanics of quantum dots differ from those of other particulate labels, the size of the crystal does not correlate with the specific activity. However, the crystal size must be slightly increased by assembling the protective cap. Similar procedure is also important in the case of inorganic phosphors. The protective layer may increase the particle size by only a few nanometers, and thereby, may exhibit only small contribution to the FRET-efficiency given a spectrally suitable FRET partner is employed. However, the most challenging aspect is to form a layer of predetermined thickness with consistency.

Overall, the ideal size of a particle in homogeneous assays is dictated by the detection principle. In FRET-based assays employing donor particles with even fluorophore distribution, the optimal particle would be of size under 50 nm in diameter due to the possibility of donor interference at the detection wavelength. However, as the thermodynamics of such particles are less favourable, core-shell-structured particles

with a thin emissive shell and diameter of approximately 100 nm would be ideal given the other characeristics also beneficial in heterogeneous assays. In other particle-based homogeneous assay technologies (LOCI, SPA), the size of the particle is not as critical, and therefore, large particles are preferred.

Summary

The size is the critical property of a particle label. Generally, it can be claimed that the small particles (2-50 nm in diameter) are favoured due to enhanced assay kinetics as dictated by the diffusivity. The enhanced kinetics also refer to the bulk interference of the particle being less obtrusive. On the other hand, the thermodynamics do not promote the employment of particles sized 2-50 nm in diameter. This means the particles in this size range are more prone to form irreversible aggregates, which is a potential disadvantage in regard to both assay performance and shelf-life. This issue may be alleviated with a carefully selected surface chemistry, although the biomolecule coating defines the aggregation tendency in practise. In the case of polymeric latex, silica or inorganic phosphor particles with even luminophore distribution, the specific activity is directly proportional to the particle size. However, the increase in specific activity along the size increase may produce high luminescence background. This issue may be especially present in FRET-based homogeneous assays wherein particles with even fluorophore distribution are employed as donors.

As the selection of a particle is always a compromise, currently the optimal particle size (polymeric latex, silica, inorganic phosphors) in bioaffinity assays is around 100 nm (50-150 nm) in diameter. In this size range, the monodispersity may be maintained, the kinetics are sufficiently fast for a practical assay, the geometries of many bioaffinity reactions allow this particle size due to the bulk not being a significant interference, and the specific activity is not excessive in homogeneous FRET-based assays (original publication V).

Given the basic ideas presented in this review, it may seem that the properties of quantum dots, or other extremely small particle labels, are not very appealing in terms of applicability to bioaffinity assays. With this aspect taken into account, the ideal quantum dots in bioaffinity application would be of size near 10 nm in diameter. This is explained by generally lower excitation energy required and the improved colloidal stability. However, in specific applications such as bioimaging, a smaller particle size is preferred due to better tissue penetration (Zimmer et al. 2006). As the photoluminescent property of gold colloids is only one of the many features exploitable in bioaffinity applications, the size is an integral parameter in terms of not only the colloidal stability but also size-dependent specialities. Hence, given the fact that gold colloids can be prepared in various sizes and shapes, the ideal size or morphology is more dependent on the application.

2.6   Future prospects of particulate labels

From the first particle-based bioaffinity assays dating back to the 1950's, (Singer and Plotz 1956) there has been a trend towards smaller particle sizes. This development has been pushed forward not only by the technical advances in the organic and inorganic chemistry or in the synthesis of functional entities close to the molecular size, but also by the special phenomena observed as the size has reached the low nanometer range. The discovery of quantum confinement effect and the consequent elaboration of quantum dots in the 1980s (Brus 1986) gave rise to a significant interest to the various forms of particulate reporters.

One could speculate whether the size development will continue further from the current state. The size of the quantum dots is already at its low limit due to the smallest crystals having the size of small biomolecules and generally exhibiting higher bandgaps than practical in bioaffinity assays. At the moment, the practical size range of other photoluminescent particles has almost reached its low-end, because given the properties of macromolecular analytes and binding molecules, smaller particles are not favoured due to the loss of solid phase-like characteristics, enhanced monovalent affinity and high specific activity originally considered as the principle assets of particulate labels. On the technical side, the particles cannot be diminished due to the thermodynamical limitations. However, the evolution of binding molecules through establishment of small molecule libraries, new particle preparation techniques and increased knowledge of materials will undoubtedly push the boundary further down the nanometer scale. Inevitably, the trend will continue until the size of a particle matches that of the small molecules. At that point, one has created a label comparable to intrinsically luminescent small molecules desirably with improved quantum properties, photostability and robustness.

Instead of the particle size decrease, it would be more beneficial to further enhance the preparation techniques to produce particles with higher colloidal stability and less batch-to-batch variation. The latter is especially the case with quantum dots, the preparation chemistry of which is extremely error-prone with respect to size deviations. This accompanied with difficult handling characteristics are the most prevalent issues halting the commercial quantum dot applications despite the significant interest. Also, room for improvement has been left in the preparation of small inorganic crystals among which up-converting phosphors have gained considerable interest in the past two decades. The ability to produce additional surface layers with functionality, i.e. inorganic-organic hybrids or core-shell particles, has been difficult to perform with consistency. Hence, it may be envisioned that such particle types will remain to be the target of developmental interest in the near future. Overall, the development of different core-shell structures seems extremely sound, as the luminescent and surface properties can be assigned deliberately, and the overall size of the particles can be adjusted irrespective of the label content.

The more efficient utilization of the particulate surfaces will also be focused on. Currently, the most common means of conjugating biomolecules onto the surface are either through covalent coupling or passive adsorption. Although these may be efficient techniques of biomolecule immobilization, the activity of the bound molecules is compromised due to the random orientation and conformation changes upon the attachment. Therefore, specific orientation of the molecules will be of great importance in order to take full advantage of the expanded surface area the particles provide. While the particulate labels already offer enhanced monovalent affinity due to the multitude of binding molecules coupled onto the surface (Soukka et al. 2001a), the affinity could be significantly increased if more control over the immobilization was provided. In this regard, the modification of binding molecules with specific moieties is already a significant tool with respect to site-specific conjugation. However, despite the advances of site-specific conjugation, to create truly homogeneous particle surfaces, the passive adsorption of molecules in the coating reaction must be prevented due to random orientation factor. Therefore, self-assembly of molecules onto the surface may be a feasible approach as well as the utilization of otherwise inert surface to molecular adhesion as already described by Huang and coworkers (2001, 2002). However, the approach described by Huang produces relatively thick surface layers due to the utilization of polyethylene glycol. Therefore, this approach may not be feasible in proximity-dependent assay techniques.

The quantum properties of photoluminescent nanoparticle reporters have already been developed for better compliancy with biomolecular environments. Compared to bioaffinity assays conducted with conventional fluorophores, time-resolved fluorometry used in conjunction with long-lifetime fluorescent nanoparticles with broad Stokes' shifts, luminophores exciteable with lower energy (Werts et al. 1999) and emitting at the red-end of the spectrum enable significantly improved assay sensitivities due to the elimination of background fluorescence. Also, the laser excitation of up-converting phosphors and the up-conversion phenomenon as a whole are highly suitable for bioaffinity assays. Despite the evolution, the quantum efficiency of e.g. lanthanide(III) complexes does not match that of the conventional fluorophores in general, although refinements in this regard have been reported (Kömpe et al. 2003). General for the inorganic crystals and quantum dots with high surface-to-volume ratio, probably the most important resort to improve quantum yields is to suppress the energy-loss at the particle surface. Therefore, the controlled construction of a passivating shell is of great importance, and the research of different material combinations in the core-shell structures will continue as to improve this aspect. In addition, the improvements of bottom-up fabrication of inorganic phosphors will also be concentrated on due to the surface imperfections induced by the grinding in the top-down approach (Beverloo et al. 1990). For the particles doped with organic luminophores, the development will be concentrated on the molecular configurations of the antenna to improve the quantum properties. The spectral properties of nanoparticle

labels will also be fine-tuned, in accordance with observations of Pires et. al (2005), to meet the specific requirements of e.g. FRET-based assays.

To conclude, while the diverse materials and techniques used for particle preparation has seen a practical overhaul in the past, the surface modifications in relation to effective utilization of the surface areas of particulate reporters has been left plenty of room for improvement. This may be partly explained by the particle preparation techniques and materials not originally designed as assets for the development of bioaffinity assays. Therefore the adjusting of the particles to be effective in biomolecular environments remains still ongoing.

3 Aims of the Study

This study focuses on different opportunities and benefits of utilizing nanoparticle labels in bioaffinity assays. The research covers the fields of conventional diagnostic (I,II) and high-throughput screening (III,IV) assays. Also, a delve into the fundamental properties of differently sized donor particles in FRET-based applications is made (V).

The focus of the original publications were:

I   To develop a highly sensitive and dynamic immunoassay for adenovirus detection from clinical nasopharyngeal specimens employing europium-chelate-doped nanoparticles. To further expand the applicability of the nanoparticles, a novel, albeit conventional immunoassay for adenovirus detection was established and compared to a routinely used reference technique.

II   To create a nanoparticle-based all-in-one immunoassay for the detection of hepatitis B surface antigen from serum specimens. The objective was the development of a one-step assay concept involving dry chemistry.

III   To prove the functionality of F(R)ET-based separation-free assay configuration employing particle–particle interaction. The study presented a novel technology concept and showed that particulate acceptors in combination with particulate donors are suitable in a non-competitive assay format. A model assay was developed for prostate-specific antigen (PSA).

IV   To prove a FRET-based separation-free assay using europium-chelate-doped nanoparticles can be established for analyzing proteolytic activity. A novel dual-step FRET concept was introduced and was presumed to be a useful alternative in the high-throughput screening of caspase-3 inhibitors.

V   To evaluate the influence of particle size on properties of a FRET-based separation-free assay using a simple protein adsorption-driven donor-acceptor pair formation. The suitability of the principle was also evaluated for analyzing protein concentrations.

4 Materials and Methods

A summary of reagents, detection instruments, methods regarding the characterization of principle assay components and assay procedures introduced in the original publications I-V is presented in the following chapters. More detailed information is found in the publications.

4.1 Europium(III)-chelate-doped nanoparticles

Europium-fluorescent FluoroMax™ nanoparticles (Seradyn Inc, IN) of sizes 47, 68, 92, 107 and 202 nm were employed throughout this study. This is a series of particles fabricated in a similar batch growth method allowing the doped tris(2-naphthoyl trifluoroacetone) europium(III)-chelate content to reflect the particle size as confirmed by Härmä et al. (2001). The content of acrylic acid copolymer in the polymerization varied from particle size to another giving them a subtly different surface charge. The density of carboxyl groups (groups per nm^2) for 47, 68, 92, 107 and 202 nm particles were 1.11, 0.96, 2.78, 1.88 and 2.94, respectively. These groups enabled the covalent coupling of binding molecules onto the surface and provided colloidal stability to the particles in suspension.

4.2 TransFluoSphere™ particles

Non-charged polystyrene TransFluoSphere™ particles (excitation/emission: 630/760 nm) of 2 µm in diameter were obtained from Molecular Probes Inc. (OR). These particles contain multiple conventional fluorophores, which enable an internal energy transfer relay and a consequent large Stokes' shift. Biomolecule conjugation onto the particle surface was carried out via passive adsorption.

4.3 Binding molecules

Monoclonal anti-adenovirus (anti-hexon) antibodies clone 2HX2 were provided by the Department of Virology (University of Turku). The same clone was used both as capture (coupled onto the microtiter well) and as detection antibody (coupled onto the nanoparticle) (I). Monoclonal anti-HBsAg IgM capture antibodies of clone 12F7-2 were obtained from Shanghai SIIC Kehua Biotech Co.Ltd. (China), and monoclonal IgG detection antibodies of clone HB11 were from HyTest Ltd. (Finland) (II). Anti-PSA IgG antibodies clones H117 and 5A10 were produced at the Department of Biotechnology (University of Turku, Finland) (III). Streptavidin was a product of BioSpa (Italy) (IV) and bovine serum albumin (BSA, fraction V) a product of Bioreba (Switzerland) (V).

4.4   Instruments

The particle fluorescence was measured with Victor 1420 multilabel counter (PerkinElmer Life and Analytical Sciences, Wallac Oy, Finland) at the europium(III) emission maximum (615 nm) using time-resolved measurement (400-µs delay and measurement window) and the filter set provided with the instrument. In homogeneous assay formats (III-V), the fluorescence of the sensitized acceptor or secondary emission emanating from the particles at 730 nm (IV,V) or 760 nm (III) was measured with a 1234 Research Fluorometer (1234-fluorometer) (Wallac Oy, Finland) modified with a red-sensitive photomultiplier tube (R2949, Hamamatsu, Japan). The instrument was also equipped with DUG11 excitation bandpass filter (340 nm) and a 730-nm (IV,V) or 760-nm (III) emission bandpass filter together with a 700-nm (IV,V) or 715-nm (III) longwave pass filter. Measurements featured a 75-µs delay and 50-/400-µs counting times. For spectrofluorometric evaluations, Cary Eclipse (Varian Inc., CA) was utilized (III,IV). Mass analyses of modified small molecule components were carried out using Voyager-DE PRO Biospectrometry Workstation (PerSeptive Biosystems/GMI, MN) (IV), and for photometric measurements, Biospec-1610E (Shimadzu, Japan) was employed (IV). All measurements carried out with plate-fluorometers (Victor 1420, 1234-fluorometer) were conducted on Low-Fluorescence MaxiSorp microtiter plates (Nunc, Denmark). In spectrofluorometric measurements, a Quartz Suprasil cuvette (Hellma Optik, Germany) was utilized.

4.5   Reagent preparations

4.5.1 Particle-conjugates

FluoroMax particles of 47 (IV,V), 68 (IV,V), 92 (V), 107 (I-III) and 202 (V) nm in diameter were employed and functionalized by attaching binding proteins (I-IV) or modified BSA (V) onto the surface via covalent coupling (I-IV) or passive adsorption (III,V).

   To promote the persistency and activity of the proteins on the particle surface, covalent coupling exploiting the protruding carboxyl moieties of the polymeric particles was carried out. This involved a two-step chemistry using EDC (N-ethyl-N'-dimethylaminopropyl carbodiimide, Fluka) and NHS (N-hydroxysuccinimide sodium salt, Fluka) for the activation of carboxyl groups to react with primary amines of the proteins. The most susceptible targets are lysine epsilon-amine groups (Hermanson 1996). Briefly, the nanoparticles (e.g. 1×10^{12} units, 107 nm particles) were washed with neutral sodiumphosphate buffer (50 mM, pH 7.0) using filtered centrifuge tubes (300 kDa cut-off, Pall, MA). The particles were resuspended into this buffer using sonication, and the activation reagents, EDC and NHS, were applied in the final concentrations of e.g. 1 mM and 10 mM, respectively. After the activation step (15 minutes at room temperature), the particles were washed with the coupling buffer. The composition of this buffer was reliant on the protein to be attached, e.g. the pH-value being a compromise between the ideal

pH-value of the NHS group and the pI-value of the protein to ensure efficient coupling. Therefore, the composition of coupling buffer had to be adjusted for different proteins individually. The particles were resuspended and mixed with the protein for at least two hours at room temperature. Thereafter, an excess of BSA was added to the suspension and the incubation was continued for ½ to 1 hour at room temperature. The particles were purified using filtered centrifuge tubes or an ultrafiltration device (Millipore, MA), and the preparation was stored with NaN_3 as preservative at room temperature or at +4 °C depending on the size of the particle.

TransFluoSphere™ particles (2 µm in diameter) used in publication III were conjugated with H117-anti-PSA antibodies using passive adsorption. The coating protocol is similar to that of the active coating only without the activation phase. Also, more emphasis was given on the reaction pH-value reflecting the pI-value of the antibody.

4.5.2 Labelling with small molecules

The monoclonal IgM antibody was conjugated with biotin using amino-reactive biotin isothiocyanate (PerkinElmer Life and Analytical Sciences, Wallac Oy, Finland) (II). The biotinylated substrate peptide for caspase-3 was conjugated with a small molecule quencher BlackBerry Quencher 650 modified with an NHS-moiety (BBQ650, Berry & Associates Inc., MI) (IV). The control substrate peptide for caspase-3 was modified with an intrinsically fluorescent europium-chelate, 2,2',2'',2'''-{[2-(4-isothiocyanatophenyl) ethylimino]-bis(methylene)bis{4-{[4-(alpha-galactopyranoxy) phenyl]ethynyl}- pyridine-6,2-diyl}bis(methylenenitrilo)}tetrakis(acetate)europium(III) (9-dentate europium chelate, von Lode et al. 2003) and a thiol-reactive Atto 612Q fluorescence quencher (Atto Tec, Germany) (IV). BSA was labelled with an NHS-derivatized Alexa Fluor™ 680 (AF680, Molecular Probes Inc., Invitrogen, OR) (V).

4.5.3 Coating of microtitration wells

The microtitration wells were coated with anti-hexon-antibodies (I), streptavidin (II) and BSA (III,IV) via passive adsorption. Herein, the coating conditions were adjusted to enable dense protein coverage, i.e. the pH-value of the reaction was dictated by the pI-value of the protein to promote hydrophobic interactions between the protein and the hydrophobic polystyrene surface (Low fluorescence MaxiSorp, Nunc). When the net-charge of the protein is close to zero, the electrostatic repulsion is minimized, which affects both the protein-surface interaction affinity and lateral repulsion between individual proteins on the surface. This enables high coverage potential despite the fact that the interaction forces may induce proteins denaturation. Briefly, the coatings were carried out in phosphate buffers at room temperature (I) or at +35 °C (II-IV) in moist conditions for two hours (I) or overnight (II-IV). Subsequently, the wells were washed and a saturation solution containing high amount of BSA (0.1% w/v) supplemented with

trehalose (3% w/v) was applied, and the incubation was continued for one hour at room temperature. The wells were aspirated, dried and stored with a desiccant at +4 °C.

4.6   Samples

Purified adenovirus particles (serotype 2), nasopharyngeal aspirates (n = 50) (I) and clinical serum samples for HBsAg analyses (II) were received from the Department of Virology (University of Turku, Finland). The samples were selected on account of predetermined analyte concentrations to comprise a balanced panel covering extreme concentrations of the analyte to facilitate comparative assay evaluations.

4.7   Characterization of particle conjugates

Binding sites of particle conjugates

The number of binding sites was determined using an excess of non-luminescent terbium(III)-chelate-labelled PSA (III) or biotin (IV). The corresponding figure for anti-hexon and anti-HBsAg nanoparticles (I,II) was not verified experimentally, only the mapping of suitable antibody pairings was conducted assuming the amount of surface-bound antibodies reflects the average number according to the previous studies carried out at our department. Briefly, after the binding of terbium-labelled PSA or biotin onto the particles, the unbound fraction was washed away using sedimentation induced by centrifugation (III) or filtered centrifuge tubes (III,IV). Thereafter, the bound terbium was enhanced using Delfia Enhancement Solution and Delfia Enhancer (PerkinElmer Life and Analytical Sciences), and the fluorescence was measured using Victor 1420 multilabel counter. The mean number of binding sites per one particle was deduced by the derived fluorescence intensities using non-coated particles and a terbium standard as controls.

Particle concentration

The concentration of particles in a preparation was determined by diluting the preparation into Triton X-100 solution (0.1% w/v), applying the solution into a microtiter plate well and comparing the detected fluorescence intensity to that of a particle standard prepared from the particle stock solution, whose concentration was reported by the manufacturer. The measurements were performed with Victor 1420 multilabel counter.

4.8   Assay principles

The non-competitive heterogeneous assays in publications I and II relied on conventional molecular sandwich formation on a microtiter plate surface. In the adenovirus assay (I), the protocol (see also Figure 11) involved a two-step incubation, wherein the analyte/sample was first applied to interact with the capture surface of the plate for 30 minutes. This was followed by a washing step and a subsequent introduction of the nanoparticle conjugates. After the

label incubation of 90 minutes, the wells were washed thoroughly, and the fluorescence was measured directly from the aspirated well surfaces using Victor 1420 multilabel counter and a measurement protocol (340/615 nm, 400/400 µs), where the excitation and detection focus was adjusted onto the well surface. In the nanoparticle-based HBsAg assay (II), an all-in-one dry chemistry concept was employed. This involved the immobilization of the biotinylated capture antibody onto the streptavidin-coated wells and the application of insulation layer to protect the capture surface from the nanoparticle conjugates applied and dried on top. The assay was comprised of a single step, where the analyte/sample solubilized other assay components. After the incubation of 30 minutes, the wells were washed and the fluorescence of the well surfaces were measured as described above.

The homogeneous assay covered in publication III featured a one- or two-step protocol, both proven feasible for the detection of PSA at low concentrations. In the one-step assay, all components were applied simultaneously into BSA-coated microtiter plate wells, whereas in the two-step protocol, the analyte was first mixed with donor or acceptor particles (30-minute incubation at room temperature), and thereafter, the acceptor or donor particles were added, respectively. After an incubation period of 60 minutes at room temperature, the sensitized emission of the acceptor particles was detected with a time-resolved measurement using the 1234-fluorometer. The assay principle is illustrated in Figure 13.
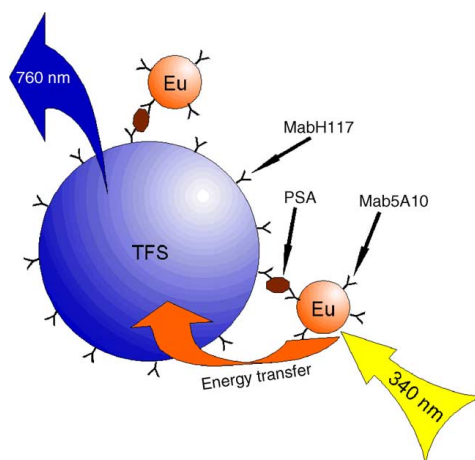

Figure 13. Principle of homogeneous PSA assay (III). Europium(III)-chelate-doped nanoparticle donors and TFS-acceptors are coated with anti-PSA-antibodies specific for distinct PSA epitopes. Particle sizes are not in proportion.

The dual-step FRET assay presented in publication IV consisted of three phases: the introduction of a compound under investigation to the enzyme (1-hour reaction at +35 °C), the addition of biotinylated substrate peptide (3-hour reaction at +35 °C), and the capture of the reaction products onto nanoparticles coated with streptavidin (45-minute reaction at room temperature). The sensitized emission of the AF680 acceptor was measured with the 1234-fluorometer. The assay principle is illustrated in Figure 14.

The adsorption studies for differently sized particles (47-202 nm in diameter), carried out in publication V, were either conducted with equal total surface area or equal total volume of particles (i.e. equal amount of particulate fluorescence, approximately 5x instrument noise at 730 nm). Because the rate of adsorption was determined as swift and similar for both the native BSA and the BSA modified with an AF680 fluorophore (BSA-AF), a short incubation period of 10 minutes was assigned for the BSA-AF. While studying the adsorption isotherms,
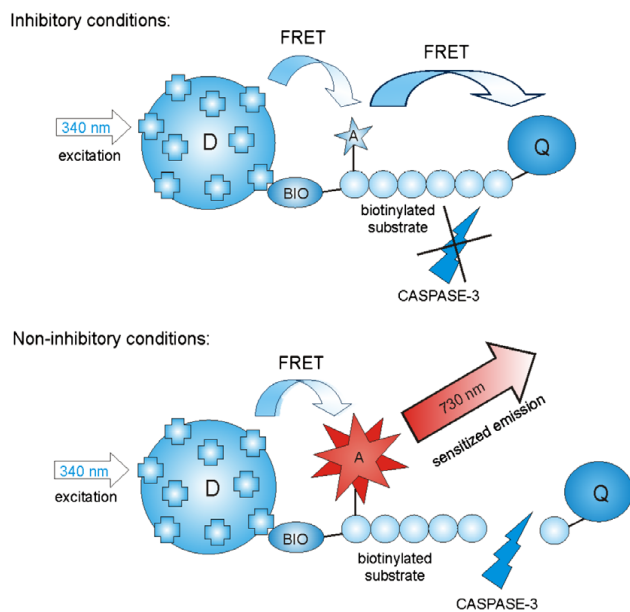
Figure 14. Principle of dual-step FRET assay for screening of caspase-3 inhibitors (IV). Streptavidin-coated europium(III)-chelate-doped nanoparticle donors (D) are excited, and the energy is transferred to the proximal AF680 acceptor (A). In inhibitory conditions, the biotinylated substrate remains intact, and the sensitized acceptor emission is attenuated by BBQ650 (Q). In non-inhibitory conditions, the enzyme cleaves the biotinylated substrate releasing BBQ650, leading to the emission of AF680 upon excitation.

different amounts of BSA-AF was mixed with differently sized particles featuring equal total surface area. BSA-AF was also used as the competitive adsorbate to determine the extent of adsorption of BSA and other proteins. The assay for protein adsorption was a two-step process, wherein varying doses of protein were first mixed with the particles of equal total volume for 20 minutes followed by the addition of BSA-AF. After the incubation period, the sensitized emission was measured using the 1234-fluorometer.

4.9 Reference assays

Some of the established nanoparticle-based assays (I,II,IV) were directly compared with commonly utilized reference tests. TR-IFMA (time-resolved immunofluorometric assay) (I) is a conventional non-competitive assay principle typically employing antibodies modified with lanthanide-chelates instead of the nanoparticle conjugates. The protocol for adenovirus detection (I) corresponds to that of the nanoparticle-based assay. The reference assay for the nanoparticle-based HBsAg assay (II) was a commercial assay kit (Enzygnost HBsAg 5.0) manufactured by Dade Behring (Germany). This ELISA was conducted according to instructions provided by the manufacturer. The reference assay in publication IV was developed according to the assay protocol and substrate structure found in literature (Karvinen et al. 2004). This was a simplified homogeneous assay principle to evaluate caspase-3 activity relying on a dual-labelled substrate (terminally labelled with 9-dentate europium chelate and Atto 612Q fluorescence quencher), whose fluorescence altered upon the enzymatic activity. After the enzymatic reaction, the intensity of Eu-fluorescence was measured. This was also used as the control assay to ensure proper enzymatic activity from one assay to another.

5   Results

It was shown that the nanoparticle-based assays for adenovirus (I) and HBsAg (II) detection provided better sensitivity, potentially a 10- to 1000-fold improvement, over the reference assays. The lowest limit of detection (LLD; analyte concentration giving the signal 3xSD above the mean signal of zero calibrator) for purified adenoviruses was determined as 5700 virus particles per one milliliter, while the respective figure for the HBsAg detection was 0.03 ng/ml (one-step assay). The improved LLDs compared to those of the reference methods were attributed to the extreme specific activity and high monovalent affinity of the nanoparticle conjugates. The better assay sensitivity and also dynamics were observed in the sample panel analyses (Table 2 and Figure 15), sample dilution profiles and calibration studies.
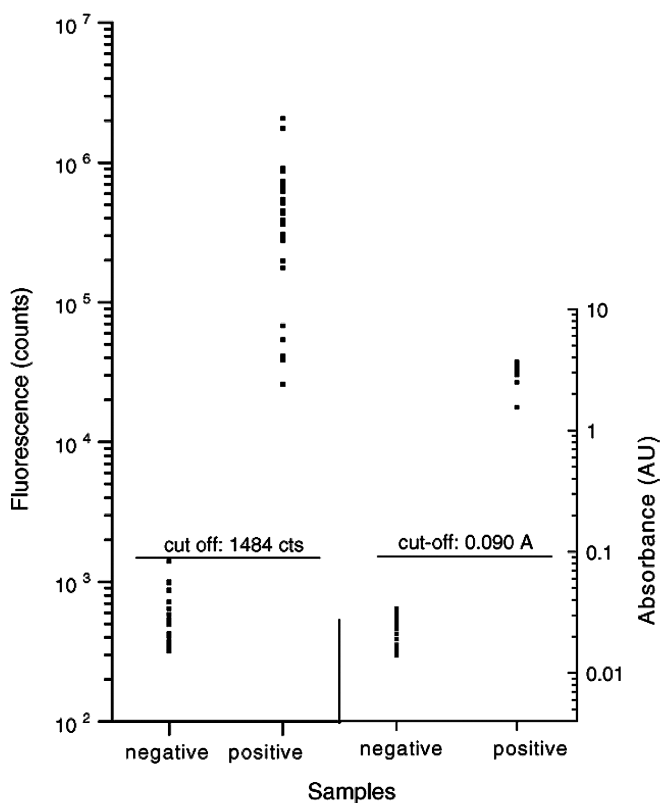
Figure 15. Analysis of 20 negative and 30 HBsAg positive serum samples using the 30-minute nanoparticle-based assay (left) and a reference assay (Enzygnost HBsAg 5.0) (right).

The performance of the homogeneous FRET-based PSA assay (III) was respectful, with very low signal variations and the LLD being < 0.1 ng/ml (two-step assay) or < 0.2 ng/ml (one-step assay) (Fig. 16). However, the assay dynamics, being similar in one- and two-step procedures, was only two orders of magnitude (0.25-25 ng/ml).

Table 2. Sensitivity comparison using positive adenovirus samples: Nanoparticle-based assay vs. TR-IFMA.

Results of the dilution test of 10 positive nasopharyngeal samples: sensitivity comparison of reference and nanoparticle-based assay

| Positive sample	TR-IFMA-counts of 1/5 dilution	S/B ratio of TR-IFMA[a]	Dilution factor of the nanoparticle assay[b]	R^2-value of linear fit[c]
1	2694	24	14	0.991
2	508413	4622	146	0.997
3	23672	215	41	0.982
4	174169	1583	38	0.999
5	1189	11	906	1.000
6	955516	8687	60	0.999
7	7186	65	–[d]	–
8	355953	3236	22	0.999
9	$>1 \times 10^6$	>9091	<61[e]	0.999
10	57210	520	33	0.989
Average			38[f]	
S.D.%			2.1[f]	

The sample volumes used in reference and nanoparticle-based assays were 50 and 40 µl, respectively.

[a] The S/B ratios of undiluted samples were calculated by using the average background signal of 550 counts.

[b] The sample dilution of the nanoparticle-based assay resulting in the same S/B ratio as in the reference method, was calculated according to linear range linear fit of the dilution series.

[c] Linear ranges of all the curves covered four to five data points.

[d] The value was excluded, because the linear range of the curve did not cover three data points.

[e] The value was excluded, because the sample exceeded the capacity of the IFMA method.

[f] The values were calculated using (1/dilution factor)-values and the results were converted to average dilution factor and percentage value.
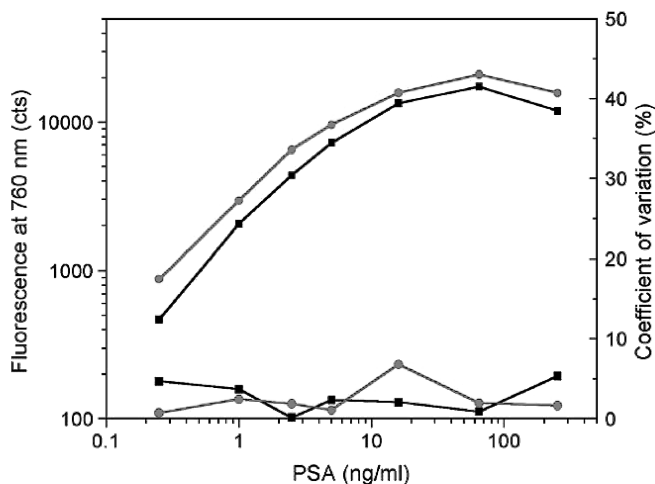
Figure 16. PSA calibration curves and precision profiles obtained from the two-step (circle) and one-step assay (square) with 90-min total incubation.

The unique dual-step FRET concept, developed for assaying caspase-3 activity with nanoparticle labels (IV), was proved feasible as the sensitized fluorescence derived from the acceptor AF680 was proportional to the activity of the enzyme. This indicates that the enzyme recognized and hydrolyzed the biotinlated substrate analogue specifically releasing the C-terminal BBQ650 from the proximity of the N-terminal AF680. Incidentally, reproducible sigmoidal inhibition curves were produced with varying amounts of irreversible caspase-3 inhibitor Z-DEVD-FMK (Fig. 17). The IC-50 value deduced (~12 nM) for the experimental setup agrees with a previous report of Gopalakrishnan et al. (2002). However, the decomposition of the BBQ650 induced by the reducing agent dithiothreitol (DTT) interfered with the assay dynamics and sensitivity. In the reference assay, a similar inhibition profile but with a significantly decreased IC-50 value (~0.05 nM) was observed (Fig. 17).
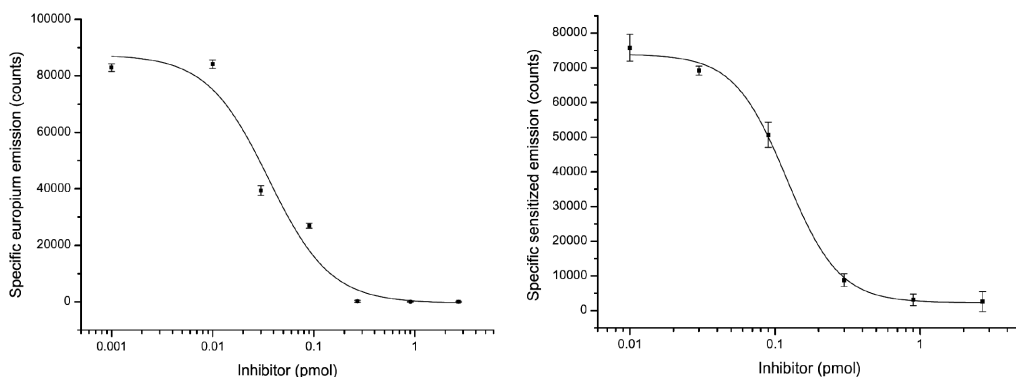

Figure 17. Nanoparticle-based dual-step FRET quenching assay (left) and reference assay response (right) to varying inhibitor (Z-DEVD-FMK) doses.

In publication V, the particle size influence on background fluorescence in a FRET-based competitive assay configuration was observed to be practically insignificant in the particle diameter range of 47 to 202 nm (Fig. 18). When the volumes of differently sized particles were aligned to evaluate the adsorption of BSA (and other proteins), i.e. the surface areas were different for each particle type, the assay properties were in agreement with the rules of a competitive assay (Fig. 19).
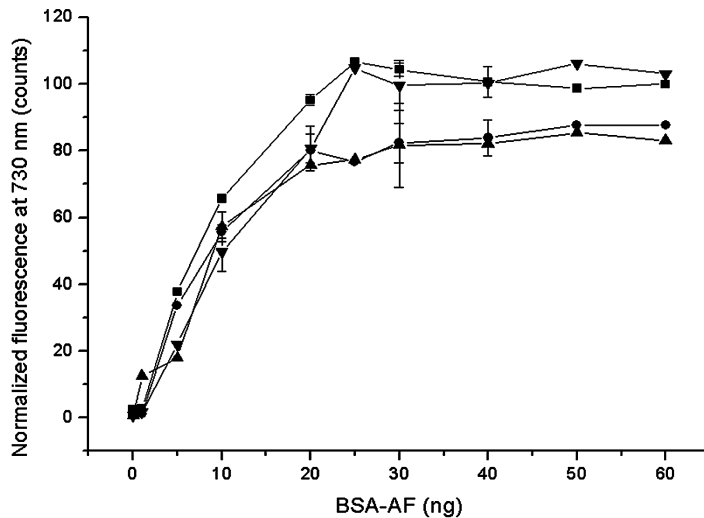
Figure 18. Adsorption isotherms for all particle sizes: 47 (down triangle), 68 (up triangle), 92 (circle), 202 nm (square) in diameter. In the experiment, the total surface areas of the particles were aligned and subjected to BSA-AF adsorption. The fluorescence values were normalized relative to the fluorescence derived from the 202 nm particles at the BSA-AF amount of 60 ng.
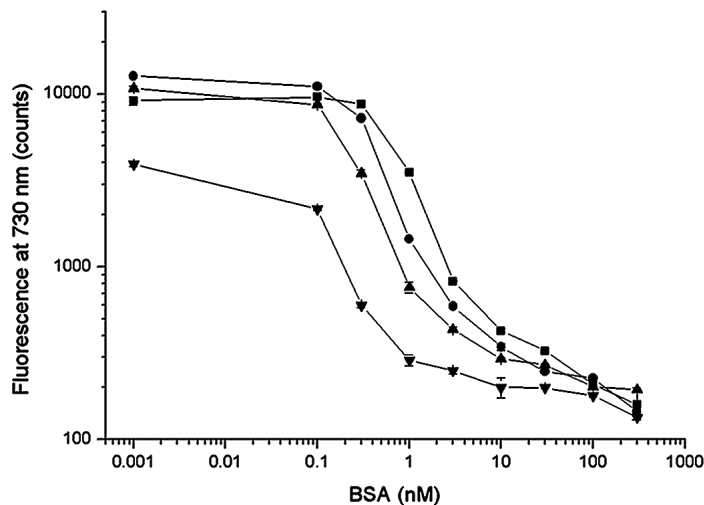
Figure 19. BSA calibration curves for different particles: 47 (square), 68 (circle), 92 (up triangle) and 202 nm (down triangle) in diameter. In the experiment, the particle volume, i.e. the particle fluorescence, was equal for all particle sizes. The sigmoidal curves reflect the displacement of BSA-AF by native BSA on the particle surfaces.

6 Discussion

6.1 Heterogeneous assays for viral analytes (I,II)

The development of nanoparticle-based heterogeneous assays for adenovirus (I) and hepatitis B surface antigen (II) were interesting not only because of the clinical importance but also due to the structure of the analytes. Especially the adenovirus hexons (240 repeating units in a single virion) but also the hepatitis B surface antigens are expressed on the surface of the virions in multiple, which was viewed as extremely suitable for developing nanoparticle-based assays with high sensitivity. This was due to the multivalent nature of not only the analyte but also the nanoparticles, owing to the property that a multitude of binding molecules can be conjugated onto the nanoparticle surface. Therefore, the high monovalent affinity of the nanoparticle bioconjugates due to multiple binding sites (Soukka et al. 2001a), was assumed to be further improved. This was speculated by the possibility of multiple concomitant contacts between the analyte and the nanoparticle conjugates given the size and the number of potential contact areas of both interacting species. Therefore, the sensitivity of the nanoparticle-based adenovirus assay (~5700 viral particles per milliliter), assessed with the calibration study, was improved by almost three orders of magnitude compared to that of the more traditional TR-IFMA method employing europium-labelled anti-hexon antibodies. The sample panel revealed that on average, the nanoparticle-based assay was 50 times more sensitive. The distinction compared to the calibration-based sensitivity improvement relates to the matrix effects of nasopharyngeal specimens and the consequent need for sample dilution into the assay buffer. Similarly to the adenovirus assay, a sensitivity improvement of 10-100-fold in the nanoparticle-based HBsAg assay compared to the reference assay (Enzygnost 5.0 HBsAg) was observed. The dynamics of both nanoparticle-based assays were at least of four orders of magnitude, which was a marked improvement especially when nanoparticle-based and reference HBsAg assays were compared. This was a result of narrow dynamic range of the spectrophotometric technique and the high binding capacity of the nanoparticle conjugates.

Overall, it was demonstrated that the nanoparticle labels are extremely suitable for the detection of viral antigens in patient specimens. This is especially the case when viral particles and virions contain multiple identical epitopes on the surface specific for the antibodies employed. However, compared to the highly sensitive PCR-based detection methods for e.g. adenovirus, the sensitivity of the nanoparticle-based assay was ~25-fold lower. On one hand though, the sensitivity is sufficient for the early detection of virus replication, on the other hand the labor-intensiveness and susceptibility to contaminations are major disadvantages of PCR-based assays. Thus, nanoparticle-based assays may be the next step forward from the traditional ELISA, which is the most common routine technique at present.

6.2 FRET-based assay for PSA employing particle-particle interaction (III)

PSA was treated solely as a model analyte for studying the particle–particle interaction. This was governed by the availability of high quality monoclonal antibodies (clones H117 and 5A10) produced for discrete PSA epitopes. The narrow dynamic range (0.25-25 ng/ml PSA) was attributed to the small number of particles, hence low binding capacity, utilized to achieve the low detection limit (< 0.1 ng/ml PSA). For comparison, the sensitivity of a heterogeneous TR-IFMA, dedicated to PSA detection (Delfia Free/Total PSA kit by PerkinElmer), was < 0.05 ng/ml. As presumed, the particle doses analyzed defined the sensitivity and dynamics of the assay, because of the donor fluorescence interference in the detection window and the binding capacity directly reflected by the particle number used. As a noteworthy observation, it was speculated that the interacting particles being large entities promoted the proximity-dependent reabsorptive energy transfer, which was considered as an unusually dominant form of acceptor sensitization in addition to the heavily distance-dependent non-radiative excitation (i.e. FRET). This speculation was established by the high level of sensitized emission observed, the lack of progressively decreasing donor emission lifetime upon immunocomplex formation and the relatively large molecular sandwich increasing the distance between donor and acceptor fluorophores beyond the imagined Förster distance (not verified experimentally). Had the reabsorption caused high non-specific background fluorescence, a feature the acceptor particles may have had due to the large size, the assay performance would have been less favorable. Therefore, the reabsorptive energy transfer was viewed as beneficial, because it was realized as mostly specific due to the proximity reliant induction. In conclusion, particulate acceptors can only be considered viable in separation-free assays, where a non-competitive format with good sensitivity is required. However, the principle is not feasible for direct competitive assays due to the large size of the particles.

6.3 Dual-step FRET assay for screening of caspase-3 inhibitors (IV)

The concept of dual-step FRET was an unprecedented approach in the field of homogeneous assay development. Also, the concept was viewed as the only feasible technique for analyzing proteolytic activity when particulate donor labels were employed. This can be explained by a number of aspects. First, the extremely high specific activity of the label prohibits the use of direct donor quenching method utilized in most of the proteolytic activity assays, because a great proportion of donor fluorophores inside the particles cannot be quenched due to the FRET-range limitation. Consequently, the setup relying on donor particle quenching would lead to a high background fluorescence in the event of maximal enzyme inhibition (the substrate-quencher conjugate intact) decreasing the sensitivity and dynamic range of the assay. Second, it was beneficial to use a secondary quencher

(BBQ650) to minimize the extent of reabsorptive excitation of the fluorescent acceptor AF680. This led to a lower background fluorescence in the event of enzyme inhibition improving the sensitivity and dynamic range, given that the substrate in an imaginable assay setup would only be modified with AF680 or other suitable acceptor fluorophore. Lastly, the principle interests of this study were established around the following aspects: i) the economical assets of employing generic nanoparticle donors in conjunction with a peptide substrate modified with commercially and readily available small molecule labels, and ii) the benefits of the nanoparticles in the effectiveness of acceptor sensitization and capture due to the high specific activity and high binding capacity.

The performance of the dual-step FRET assay for screening of caspase-3 inhibitors proved to be in good agreement with a previous report (Gopalakrishnan et al. 2002) indicating that the technique could be feasible for in vitro –screening studies. However, probably the most critical performance hallmarks, the resolution of highly inhibitive compounds and the dynamic range of the assay in general, left room for significant improvement. This was caused by the loss of quenching properties of the BBQ650 induced by the reducing agent DTT required in the enzymatic reaction. Therefore, the calculated signal-to-background ratio, i.e. the sensitized emission upon 100% enzyme activity divided by the emission upon 100% enzyme inhibition, did not compare well with that of e.g. the TruPoint assay (PerkinElmer Life and Analytical Sciences). The assay dynamics and the resolution of compounds possessing high inhibition degrees can be critically improved by selecting the label combination compatible with the caspase-3-optimized reaction buffer. However, the proposed label setup could be applicable to an inhibitor screening assay for other proteolytic enzymes not requiring DTT.

Another feature leaving space for further development would be the multi-stage assay protocol. As such, the assay is comprised of three steps, which sets high demands if automation is to be implemented. A simplified assay of mix-and-measure concept would be more desirable, especially in high-throughput screening. With the suggested assay configuration this is challenging due to the bulk of the particles causing potential steric hindrance to the enzyme, if the substrate attaches onto the surface of the particle prior to the enzyme recognition. Thus the amino acid sequence may become unavailable to the enzyme due to the proximity of the particle. A possible resort to circumvent the problem would be the introduction of binders specific for a terminal amino acid sequence that is exposed only after the hydrolyzation by the enzyme. Coating the particles with such binders would enable a true nanoparticle-based one-step assay for the inhibitor screening of proteolytic enzymes.

The decreased IC-50 value of the reference assay indicated that the affinity of the enzyme towards the control substrate was substantially decreased. Hence it may be suggested that a screening assay with increased inhibitor sensitivity would be developed if a substrate-

enzyme recognition was deliberately hindered. This could be accomplished with a targeted alteration to the amino acid backbone or by introducing specific modifications to the substrate terminals.

6.4   Size effect of donor particles on FRET-based assay (V)

Originally, the size effect was studied to support my own views on particle-based FRET. Thus, the performance of differently sized particles in a competitive FRET-based assay was evaluated. The results indicate, that contrary to the previous estimations of my own and others (e.g. Meyer et al. 2003), the sensitivity of an assay was not critically affected when the particle size was increased (47-202 nm). This was at least partly attributed to the detection wavelength utilized (730 nm), where the emission of europium donor is at its minimum. In the previous estimations, the optimal size of < 50 nm in diameter for a donor particle was proposed, because of the FRET-range limitation. In theory, this is correct, given the Förster theory and the fluorophores residing outside the energy transfer range causing background fluorescence if high donor emission at the detection wavelength occurs (see also Figure 12). However in practice, the fraction of donor europium(III) fluorophores outside the FRET-range was too small to expose a significant background fluorescence in the experimental setup, when the donor particle number was adjusted to match the practical binding capacity in assays. In addition to the ideal detection wavelength, the low background fluorescence emanating from the particle cores was heavily overshadowed by the sensitized emission. Hypotetically however, by selecting a donor particle sized far beyond the 202 nm in diameter, the largest particle employed in the study, the background fluorescence issue would be inflicted due to the exceedingly high number of donor fluorophores residing outside the effective FRET range. The results of this study propose, that the properties of a competitive assay relying on FRET and particulate donors can be adjusted by selecting a properly sized particle with suitable surface characteristics. The particle may be selected on account of sensitivity and dynamic range requirements of the assay to be developed. However, the hydrophobicity of a molecular binder on the particle surface also dictates the suitable particle size, possibly favouring the utilization of larger particles due to the improved colloidal stability over the smaller particles.

It was also proven that the competitive adsorption technique can be employed as a sensitive method for protein quantification. This was shown with different proteins (thyroglobulin, ovalbumin, gamma-globulin and BSA) with the results indicating a 100- to 1000-fold sensitivity improvement over the traditional photometric methods such as Bradford's, Lowry's and BCA techniques. The most interesting feature of this technique of protein quantification is the enhanced control over assay sensitivity and dynamics by adjusting the nanoparticle amount, and hence, the reactive surface area in reaction.

7　Summary and Conclusions

Summaries of each publication are presented below.

I　A heterogeneous nanoparticle-based non-competitive immunoassay for the detection of adenoviruses in clinical specimens was developed. Due to the labor-intensiveness of the PCR-based techniques, it was preferable to establish a nanoparticle-based assay on antigen recognition. It was observed that the multivalency of the virions improved the assay dynamic range and detection limit compared to that of the TR-IFMA reference method. With the developed assay, the number of virions detectable per one millilitre was ~5700, nearly three orders of magnitude lower than that of the reference method as determined with buffer-based calibrators. The dynamic range was at least four orders of magnitude with excellent correlation. The nasopharyngeal specimens revealed that a dilution into the reaction buffer was necessary to achieve the lowest variations due to the mucus interfering with the specific immunoreaction and sporadic samples, whose virion number exceeded the binding capacity of the nanoparticles utilized. The panel of samples revealed however, that the qualitative results completely agreed with those of the reference assay. The positive impact of nanoparticles on assay sensitivity was attributed to the high monovalent affinity resulting from two multivalent reactants allowing multiple concomitant interactions.

II　An all-in-one immunoassay for the detection of HBsAg was developed with the emphasis in high sensitivity and rapid and easy execution fulfilling point-of-care testing prerequisites. Dry chemistry was employed to prepare wells containing all integral assay components, the capture antibodies and the nanoparticle conjugates, and to preserve their functionality. The one-step execution included the addition of sample, incubation and a washing step prior to the time-resolved measurement of the surface-bound nanoparticles. The experiments with buffer-based calibrators revealed the LLD of 0.03 ng/ml HBsAg and the dynamic range of 0.1-100 ng/ml HBsAg using a 30-minute incubation period. With a 10-minute inbubation, the respective values were 0.09 ng/ml and 0.1-1000 ng/ml emphasizing the kinetic assay format. The results from serum sample evaluation and sample dilution comparisons to a routinely used reference assay (Enzygnost 5.0 HBsAg) revealed the improved dynamics of the nanoparticle-based assay. This was attributed to both the binding capacity of the nanoparticles and the detection technique being fluorometric rather than photometric. Qualitatively, the results of the sample panel were in 100% agreement with those of the reference method promoting the feasibility of the developed method.

III   A separation-free FRET-based assay principle employing particulate donors and acceptors with PSA as a model analyte was developed. With the preceding studies focusing on small molecule acceptors in conjunction with europium(III) donor nanoparticles, particulate acceptors were evaluated. Contrary to the case of small molecule acceptors, it was proposed that proximity-induced reabsorptive energy transfer was a major contributor to the overall fluorescence of the acceptor in this experimental setup. The optimized assay for the detection of PSA in buffer-based samples revealed a respectful LLD of < 0.1 ng/ml PSA. The performance was marred with a narrow dynamic range (0.25-25 ng/ml) due to the low particle number selected to obtain the high sensitivity. As a homogeneous technique, this principle is adoptable to high-throughput screening studies where a non-competitive assay of good sensitivity is required.

IV   A dual-step FRET-based assay for screening of caspase-3 inhibitors was developed. This assay relied on streptavidin-coated europium(III) nanoparticles and a biotinylated substrate, whose N-terminus was modified with AF680–acceptor fluorophore and C-terminus with an acceptor quencher BBQ650. The assay consisted of three steps: the reaction of potential inhibitor compound with the enzyme, the reaction of the biotinylated substrate with the enzyme and the capture of the biotinylated substrate onto the streptavidin-coated nanoparticles. Owing to the dual-labelled substrate, the sensitized fluorescence measured was proportional to the enzymatic activity. More importantly, the acceptor fluorescence induced by reabsorptive excitation, a potential background fluorescence contributor when particulate donors are employed, was minimized in the event of complete enzyme inhibition. The inhibition profile using a known caspase-3 inhibitor Z-DEVD-FMK was in good agreement with previous findings in the literature. However, the incompatibility of the substrate label combination with the reaction conditions restrained the performance from reaching its full potential. Overall, this principle, in which all the substrates were to be captured onto the nanoparticles, was viewed as the only feasible approach to develop a nanoparticle-based assay for a proteolytic enzyme.

V   The study focused on the influence of europium(III) particle size on the performance of a competitive FRET-based assay using protein adsorption-mediated FRET-pair formation. It was unveiled, that in the particle size range studied (47-202 nm in diameter), the size does not play a critical role in terms of the extent of background fluorescence emanating from the donor fluorophores not participating in FRET, i.e. from the core-localized fluorophores. This was explained by the fact that even though there was a subtle background fluorescence increase proportional to the particle size when no acceptor was present, the core-related background fluorescence of the donors was comprehensively overshadowed by the sensitized

fluorescence when using practical particle and acceptor amounts. Also, the reabsorptive excitation of acceptors did not prove to be significant for different particles. This was observed as the similar level of sensitized fluorescence for each particle size in the adsorption isotherm experiment, where the total surface area for each particle size was aligned. This observation is at least partly attributed to the detection wavelength (730 nm) being at the minimum of the donor emission. The results facilitate the designing of FRET-based separation-free assays utilizing particulate donors. The principle is also applicable to determine the concentration of proteins with high sensitivity as elucidated with thyroglobulin, ovalbumin and gamma-globulin.

Acknowledgements

My sincere gratitude goes to my supervisor Professor Timo Lövgren, who has given me the opportunity to work at our department and shown a persistent belief in my work and perhaps my untapped potential. In addition, I cannot stress enough the importance of the practical supervision of Dr Harri Härmä and Dr Tero Soukka, who constantly gave me fantastic ideas for my research and supported me when gasping at an insurmountable task. Without them and their jaw-dropping expertise, I would probably be lost somewhere in the midst of a never-ending post-graduate phase.

I wish to thank Professor Timo Hyypiä and Professor Heikki Tenhu for reviewing this thesis in a short notice. Their valuable comments are greatly appreciated.

I would also like to thank all my co-authors, Professor Timo Lövgren, Dr Harri Härmä, Dr Tero Soukka, Dr Pauliina Niemelä, Dr Raija Vainionpää, Dr Jouko Peltonen, Dr Pekka Hänninen, Saila Huopalahti, Hanne Lindroos, Janne Suojanen, Päivi Malmi and Heidi Appelblom for their contribution to the original publications. Saila and Päivi are worthy of a special honour for conducting the majority of practical work for the publications I, II and IV. Cheers for the excellent job.

Although I have not probably been the most go-to guy at our department, I would be half-hearted not to appreciate the easy atmosphere created by my colleages and other personnel. These include Aura Aalto, Sultana Akter, Riikka Arppe, Eeva-Cristine Brockmann, Emilia Engström, Heidi Hautala, Dr Jukka Hellman, Tuomas Huovinen, Juuso Huusko, Heidi Hyytiä. Mirja Jaala, Erik Jokisalo, Etvi Juntunen, Marja-Leena Järvenpää, Ulla Karhunen, Marja-Liisa Knuuti, Dr Leena Kokko, Tiina Kokko, Dr Katri Kuningas, Pirjo Laaksonen, Dr Urpo Lamminmäki, Ari Lehmusvuori, Janne Leivo, Päivi Malmi, Marja Maula, Merja Mustonen, Tiina Myyryläinen, Katja Niemelä, Ilari Niemi, Mari Peltola, Susan Pérez, Professor Kim Pettersson, Pirjo Pietilä, Henna Päkkilä, Terhi Rantanen, Maria Rissanen, Noora Ristiniemi, Jaana Rosenberg, Teppo Salminen, Martti Sointusalo, Henri Sund, Joanna Tynjälä, Yvette Van Der Eijk, Qi Wang, Leila Varjonen, Markus Vehniäinen, Saara Wittfooth, Johanna Vuojola, Dr Lasse Välimaa, Riina-Minna Väänänen and Minna Ylihärsilä. A special appreciation goes to Juuso, Erik and Ari, who provided me with the invigorating opportunity to chat about the essentials of life. I feel such pep-talk in disguise ought to be a privilege of everyone. An honourable mention goes to Aura and Päivi for their show of great proficiency and co-operation under my supervision.

References

Abad JM, Mertens SFL, Pita M, Fernández VM, Schiffrin DJ (2005) Functionalization of thioctic acid-capped gold nanoparticles for specific immobilization of histidine-tagged proteins, J Am Chem Soc 127: 5689.

Ackerson CJ, Jadzinsky PD, Jensen GJ, Kornberg RD (2006) Rigid, specific, and discrete gold nanoparticle/antibody conjugates, J Am Chem Soc 128: 2635.

Ahn JS, Choi S, Jang SH, Chang HJ, Kim JH, Nahm KB, OH SW, Choi EY (2003) Development of a point-of-care assay system for high-sensitivity C-reactive protein in whole blood, Clin Chim Acta 332: 51.

André A, Henry F (1998) "Emulsifier-free" emulsion copolymerization of styrene and butylacrylate: particle size control with synthesis parameters, Colloid Polym Sci 276: 1061.

Aubin M-E, Morales DG, Hamad-Schifferli K (2005) Labeling ribonuclease S with a 3 nm Au nanoparticle by two-step assembly, Nano Letters 5: 519.

Aubin-Tam M-E, Hamad-Schifferli K (2005) Gold nanoparticle-cytochrome c complexes: the effect of nanoparticle ligand charge on protein structure, Langmuir 21: 12080.

Aubin-Tam M-E, Hamad-Schifferli K (2008) Structure and function of nanoparticle-protein conjugates, Biomed Mater 3: 1.

Auzel F (2002) Up-conversion in rare-earth-doped systems: past, present and future, Proc SPIE – Int Soc Opt Eng 4766: 179.

Bagwe RP, Hilliard LR, Tan W (2006) Surface modification of silica nanoparticles to reduce aggregation and nonspecific binding, Langmuir 22: 4357.

Bailey RE, Nie S (2003) Alloyed semiconductor quantum dots: tuning the optical properties without changing the particle size, J Am Chem Soc 125: 7100.

Bazzi R, Flores MA, Louis C, Lebbou K, Zhang W, Dujardin C, Roux S, Mercier B, Ledoux G, Bernstein e, Perriat P, Tillement O (2004) Synthesis and properties of europium-based phosphors on the nanometer scale: Eu_2O_3, Gd_2O_3:Eu, and Y_2O_3:Eu, J Colloid Interface Sci 273: 191.

Bernard A, Michel B, Delamarche E (2001) Micromosaic immunoassay, Anal Chem 73: 8.

Berson SA and Yalow RS (1959) Assay of plasma insulin in human subjects by immunological methods, Nature 184: 1648.

Beverloo HB, van Schadewijk A, van Gelderen-Boele S, Tanke HJ (1990) Inorganic phosphors as new luminescent labels for immunocytochemistry and time-resolved microscopy, Cytometry 11: 784.

Beverloo HB, van Schadewijk A, Ziljmans HJMAA, Tanke HJ (1992), Immunochemical detection of proteins and nucleic acids on filters using small luminescent inorganic crystals as markers, Anal Biochem 203: 326.

Boekx RL (1984) Chemiluminescence: Applications for the clinical laboratory, Hum Pathol 15: 104.

Bower CK, Sananikone S, Bothwell MK, MacGuire J (1999) Activity losses among T4 lysozyme charge variants after adsorption to colloidal silica, Biotech Bioengin 64: 373.

Boyd GT, Yu ZH, Shen YR (1986) Photoinduced luminescence from the noble metals ant its enhancement on roughened surfaces, Phys Rev B 33: 7923.

Brennan JL, Hatzakis NS, Tshikhudo TR, Dirvianskyte N, Razumas V, Patkar S, Vind J, Svendsen A, Nolte RJM, Rowan AE, Brust M (2006) Bionanoconjugation via click chemistry: the creation of functional hybrids of lipases and gold nanoparticles, Bioconj Chem 17: 1373.

Brinkley M (1992) A brief survey of methods for preparing protein conjugates with dyes, haptens and crosslinking reagents, Bioconj Chem 3: 2.

Broach JR, Thorner J (1996) High-throughput screening for drug discovery, Nature 384 (6604 suppl): 14.

Brown K, Fox AP, Natan M (1996) Morphology-dependent electrochemistry of cytochrome *c* at Au colloid-modified SnO_2 electrodes, J Am Chem Soc 118: 1154.

Brus LE (1986) Electronic wave functions in semiconductor clusters: experiment and theory, J Phys Chem 90: 2555.

Brus LE (1983) A simple model for the ionization potential, electron affinity, and aqueous redox potentials of small semiconductor crystallites, J Chem Phys 79: 5566.

Brus LE (1991) Quantum crystallites and nonlinear optics, Appl Phys A 53: 465.

Brust M, Walker M, Bethell D, Schifrin DJ, Whyman R (1994) Synthesis of thiol-derivatised gold nanoparticles in a two-phase Liquid–Liquid system, J Chem Soc Chem Commun 801.

Chan WCW, Nie S (1998) Quantum dot bioconjugates for ultrasensitive nonisotopic detection, Science 281: 2016.

Chen M-Q, Serizawa T, Kishida A, Akashi M (1999) Graft copolymers having hydrophobic backbone and hydrophilic branches. XXIII. Particle size control of poly(ethylene glycol)-coated polystyrene nanoparticles prepared by macromonomer method, J Polym Sci A: Polym Chem 37: 2155.

Clarke L, Wybourne MNm Brown LO, Hutchison JE, Yan M, Cai SX, Keana JFW (1998) Room-temperature coulomb-blockade-dominated transport in gold nanocluster structures, Semicond Sci Technol 13: A111.

Corstjens PLAM, Li S, Zuiderwijk M, Kardos K, Abrams WR, Niedbala RS, Tanke HJ (2005) Infrared up-converting phosphors for bioassays, IEE Proc Nanobiotechnol 152: 64.

Dabbousi BO, Rodriguez-Viejo J, Mikulec FV, Heine JR, Mattousi H, Ober R, Jensen KF, Bawendi MG (1997) Core-shell quantum dots: synthesis and characterization of a size series of highly luminescent nanocrystallites, J Phys Chem 101: 9463.

Darwent JR, Porter G (1981) Photochemical hydrogen production using cadmium sulphide suspensions in aerated water, J Chem Soc Chem Commun 145.

Davies C (2001) Introduction to immunoassay principles, In The immunoassay handbook, ed. Wild D. Nature Publihing Group, London, UK.

De Roe C, Courtoy PJ, Baudhuin P (1987) A model of protein-colloidal gold interactions, J Histochem Cytochem 35: 1191.

Dequaire M, Degrand C, Limoges B (2000) An electrochemical metalloimmunoassay based on a colloidal gold label, Anal Chem 72: 5521.

Diamandis EP (1990) Analytical methodology for immunoassays and DNA hybridization assays – current status and selected systems – critical review, Clin Chim Acta 194: 19.

Diamandis EP (1992) Europium and terbium chelators as candidate substrates for enzyme-labelled time-resolved fluorimetric immunoassays, Analyst 117: 1879.

Diamandis EP (1991) Multiple labeling and time-resolvable fluorophores, Clin Chem 37: 1486.

Diamandis EP (1988) Immunoassays with time-resolved fluorescence spectroscopy: principles and applications, Clin Biochem 21: 139.

Ehrenberg M, Rigler R (1974) Rotational brownian motion and fluorescence intensity fluctuations, Chem Phys 4: 390.

Ekins RP (1960) The estimation of thyroxine in human plasma by an electrophoretic technique, Clin Chim Acta 5: 453.

Ekins RP (1987) An overview of present and future ultrasensitive non-isotopic immunoassay development, Clin Biochem Revs 8: 12.

Ekins RP, Chu F (1994), Developing multianalyte assays, Trends in Biotech 12: 89.

Ekins RP (1997) Immunoassay design and optimization, In Principles and practise of immunoassay, Ed. Price CP, Newman DJ, Macmillan Reference Ltd., London UK 173.

Ekins RP, Dakubu S (1985) The development of high sensitivity pulsed light, time-resolved fluoroimmunoassays, Pure Appl Chem 57: 437.

Elgersma AV, Zsom RLJ, Lyklema J (1990) The adsorption of bovine serum albumin on positively and negatively charged polystyrene lattices, J Colloid Interface Sci 138: 145.

Elgersma AV, Zsom RLJ, Lyklema J, Norde W (1992) Adsorption competition between albumin and monoclonal immuno-gamma-globulins on polystyrene lattices, J Colloid Interface Sci 152: 410.

Ellington AD, Szostak JW (1990) *In vitro* selection of RNA molecules that bind specific ligands, Nature 346: 818.

Elson EL, Magde D (1974) Fluorescence correlation spectroscopy. I. Conceptual basis and theory, Biopolymers 13: 1.

Engvall E, Perlmann P (1971) Enzyme-linked immunosorbent (ELISA) quantitative assay of immunoglobulin G, Immunochemistry 8: 871.

Ernst LA, Gupta RK, Mujumdar RB, Waggoner AS (1989) Cyanine dye labeling reagents for sulfhydryl groups, Cytometry 10: 3.

Evangelista RA, Pollak A, Allore B, Templeton AF, Morton RC, Diamandis EP (1988) A new europium chelate for protein labelling and time-resolved fluorometric applications, Clin Biochem 21: 173.

Eychmüller A, Katsikas L, Weller H (1990) Photochemistry of semiconductor colloids. 35. Size separation of colloidal cadmium sulfide by gel electrophoresis, Langmuir 6: 1605.

Fair BD, Jamieson AM (1980) Studies of protein adsorption on polystyrene latex surfaces, J Colloid Interface Sci 77: 525.

Faraday M (1857) The Bakerian lecture: experimental relations of gold (and other metals) to light, Phil Trans R Soc London 147: 145.

Feng J, shan G, Maquieira A, Koivunen ME, Guo B, Hammock BD, Kennedy IM (2003) Functionalized europium oxide nanoparticles used as a fluorescent label in an immunoassay for atrazine. Anal Chem 75: 5282.

Frank DS, Sundberg MW (1981a) Fluorescent labels, US Patent 4,259,313.

Frank DS, Sunberg MW (1981b) Fluorescent labels comprising rare earth chelates, US Patent 4,283,382.

Frens G (1973) Controlled nucleation for the regulation of the particle size in monodisperse gold suspensions, Nat Phys Sci 241: 20.

Förster T (1948) Zwischenmolekulare energiewanderung und fluoreszenz, Ann Physik 437: 55.

Ganapathiappan S, Zhou Z-L (2006) Maleimide-containing latex dispersions, US Patent 20080085950 A1.

Gessner A, Lieske A, Paulke B-R, Müller RH (2002) Functional groups on polystyrene model nanoparticles: influence on protein adsorption, J Biomed Mat Res Part A 65A: 319.

Gopalakrishnan SM, Karvinen J, Kofron JL, Burns DJ, Warrior U (2002) Application of micro arrayed compound screening (µARCS) to identify inhibitors of caspase-3, J Biomol Screen 7: 317.

Grabowski J, Gantt E (1978) Photophysical properties of phycobiliproteins from phycobilisomes: fluorescence lifetimes, quantum yields, and polarization spectra, Photochem Photobiol 28: 3945.

Green NM (1990) Avidin and streptavidin, Methods Enzymol 184: 51.

Hai X, tan M, Wang G, Ye Z, Yuan J, Matsumoto K (2004) Preparation and a time-resolved fluoroimmunoassay application of new europium fluorescent nanoparticles, Anal Sci 20: 245.

Hainfeld JF, Powell RD (2000) New frontiers in gold labeling, J Histochem Cytochem 48: 471.

Hainfeld JF, Liu W, Halsey CMR, Freimuth P, Powell RD (1999) Ni-NTA-gold clusters target His-tagged proteins, J Struct Biol 127: 185.

Han M, Gao X, Su JZ, Nie S (2001) Quantum-dot-tagged microbeads for multiplexed optical coding of biomolecules, Nat Biotechnol 19: 631.

Hart HE, Greenwald EB (1979) Scintillation proximity assay (SPA) – A new method of immunoassay: direct and inhibition mode detection with human albumin and rabbit antihuman albumin, Mol Immunol 16: 265.

Haugland RP (1995) Handbook of fluorescent probes and research chemicals, Molecular Probes, Eugene, OR, Ed. 6.

Hayatt MA (1989) Colloidal gold principles, Methods and applications, Academic Press, San Diego.

Hemmilä I, Dakubu S, Mukkala V-M, Siitari H, Lövgren T (1984) Europium as a label in time-resolved immunofluorometric assays, Anal Biochem 137: 335.

Hemmilä I (1988) Lanthanides as probes for time-resolved fluorometric immunoassays, Scand J Clin Lab Invest 48: 389.

Hemmilä I (1985) Fluoroimmunoassays and immunofluorometric assays, Clin Chem 31: 359.

Henglein A (1988) Mechanism of reactions on colloidal microeletrodes and size quantization effects, Top Curr Chem 88: 369.

Hermanson GT (1996) Bioconjugate techniques, Academic Press.

Ho D, Chu B, Lee H, Montemagno CD (2003) Directed protein orientation by site-specific labeling, IEEE Nano Conference 2003, San Francisco, CA, accessed via internet on the 13th of October 2008: http://ieeenano2003.arc.nasa.gov/THM3.pdf

Horisberger M (1979) Evaluation of colloidal gold as a cytochemical marker for transmission and scanning electron microscopy, Bio Cell 36: 253.

Hou X, Liu B, Deng X, Zhang B, Yan J (2007) Monodisperse polystyrene microspheres by dispersion copolymerization of styrene and other vinyl comonomers: characterization and protein adsorption properties, J Biomed Mat Res Part A 280.

Hu M, Qian L, Briñas RP, Lymar ES, Hainfeld JF (2007) Assembly of nanoparticle-protein binding complexes: from monomers to ordered arrays, Angew Chem Int Ed 46: 5111.

Huang N-P, Vörös J, De Paul SM, Textor M, Spencer ND (2002) Biotin-derivatized poly(L-lysine)-g-poly(ethylene glocol): a novel polymeric interface for bioaffinity sensing, Langmuir 18: 220.

Huang N-P, Michel R, Vörös J, Textor M, Hofer R, Rossi A, Elbert DL, Hubbell JA, Spencer ND (2001) Poly(L-lysine)-g-poly(ethylene glycol) layers on metal oxide surfaces: surface analytical characterization and resistance to serum and fibrinogen adsorption, Langmuir 17: 489.

Huhtinen P, Kivelä M, Kuronen O, Hagrén V, Takalo H, Tenhu H, Lövgren T, Härmä H (2005) Synthesis, characterization and application of Eu(III), Tb(III), Sm(III), and Dy(III) lanthanide chelate nanoparticle labels, Anal Chem 77: 2643.

Huignard A, Gacoin T, Boilot J-P (2000) Synthesis and luminescence properties of colloidal YVO_4:Eu phosphors, Chem Mater 12: 1090.

Härmä H, Lehtinen P, Takalo H, Lövgren T (1999) Immunoassay on a single microparticle: the effect of particle size and number on a miniaturized time-resolved fluorometric assay of free prostate-specific antigen, Anal Chim Acta 387: 11.

Härmä H, Soukka T, Lövgren T (2001) Europium nanoparticles and time-resolved fluorescence for ultrasensitive detection of prostate-specific antigen, Clin Chem 47: 3.

Irvine AD, Sun P, Kos L, Wang XQ, Paller AS (2002) A colorimetric bead-binding assay for detection of intermolecular interactions, Exp Derm 11: 462.

Isobe H, Kaneko K (1999) Porous silica particles prepared from silicon tetrachloride using ultrasonic spray method, J Colloid Interface Sci 212: 234.

Jackson AM, Myerson JW, Stellacci F (2004) Spontaneous assembly of subnanometre-ordered domains in the ligand shell of monolayer-protected nanoparticles, Nat Mater 3: 330.

Karvinen J, Elomaa A, Mäkinen M-L, Hakala H, Mukkala V-M, Peuralahti J, Hurskainen P, Hovinen J, Hemmilä I (2004) Caspase multiplexing: simultaneous

homogeneous time-resolved quenching assay (TruPoint) for caspases 1, 3, and 6, Anal Biochem 325: 317.

Kim SH, Jeyakumar M, Katzenellenbogen JA (2007) Dual-mode fluorophore-doped nickel nitrilotriacetic acid-modified silica nanoparticles combine histidine-tagged protein purification with site-specific fluorophore labeling, J Am Chem Soc 129: 13254.

Kohler G, Milstein C (1975) Continuous cultures of fused cells secreting antibody of predefined specificity, Nature 256: 495.

Kokko L, Sandberg K, Lövgren T, Soukka T (2004) Europium(III) chelate-dyed nanoparticles as donors in a homogeneous proximity-based immunoassay for estradiol, Anal Chim Acta 503: 155.

Kokko L, Lövgren T, Soukka T (2007) Europium(III)-chelates embedded in nanoparticles are protected from interfering compounds present in assay media, Anal Chim Acta 585: 17.

Kondo A, Murakami F, Kawagoe, M, Higashitani K (1993) Kinetic and circular dichroism studies of enzymes adsorbed on ultrafine silica particles, Appl Microbiol Biotechnol 39: 726.

Konterman R (2005) Site-specific coupling of polypeptides, Patent WO/2005/070960.

Kortesuo P, Ahola M, Kangas M, Yli-Urpo A, Kiesvaara J, Marvola M (2001) In vitro release of dexmedetomodine from silica xerogel monoliths: effect of sol-gel synthesis parameters, Int J Pharm 221: 107.

Kricka LJ (1994) Selected strategies for improving sensitivity and reliability of immunoassays, Clin Chem 40: 347.

Kricka LJ (1993) Ultrasensitive immunoassay tehcniques, Clin Biochem 26: 325.

Kricka LJ (1996) Strategies for immunoassay, Pure Appl Chem 68: 1825.

Kömpe K, Borchert H, Storz J, Lobo A, Adam S, Möller T, Haase M (2003) Green-emitting CePO$_4$:Tb/LaPO$_4$ core-shell nanoparticles with 70 % photoluminescence quantum yield, Angew Chem Int Ed 42: 5513.

Laitala V, Hemmilä I (2005) Homogeneous assay based on anti-Stokes' shift time-resolved fluorescence resonance energy-transfer measurement, Anal Chem 77: 1483.

Laporte O, Meggers WF (1925) Some rules of spectral structure, J Opt Soc Am 11: 459.

Laukkanen ML, Orellana A, Keinänen K (1995) Use of genetically engineered lipid-tagged antibody to generate functional europium chelate-loaded liposomes: application in fluoroimmunoassay, J Immunol Methods 185: 95.

Lehn JM (1978) Cryptates: the chemistry if macropolycyclic inclusion complexes, Acc Chem Res 11: 49.

Leif RC, Thomas RA, Yopp TA, Watson BD, Guarino VR, Hindman DH, Lefkove N, Vallarino LM (1977) Development of instrumentation and fluorochromes for automated multiparameter analysis of cells, Clin Chem 23: 1492.

Li S, Hu J, Liu B (2005) A study on the adsorption behaviour of protein onto functional microspheres, J Chem Technol Biotechnol 80: 531.

Link S, El-Sayed MA (2000) Shape and size dependence of radiative, non-radiative and photothermal properties of gold nanocrystals, Int Revs Phys Chem 19: 409.

Liu B, Cao S, Deng X, Li S, Luo R (2006) Adsorption behaviour of protein onto siloxane mocrospheres, Appl Surface Sci 252: 7830.

Liu G, Lin Y (2005) A renewable electrochemical magnetic immunosensor based on gold nanoparticle labels, J Nanosci Nanotechnol 5: 1060.

Lundqvist M, Nygren P, Jonsson B-H, Broo K (2006) Induction of structure and function in a designed peptide upon adsorption on a silica nanoparticle, Angew Chem Int Ed 45: 8169.

Lück M, Paulke B-R, Schröder W, Blunk T, Müller RH (1998) Analysis of plasma protein adsorption on polymeric nanoparticles with different surface characteristics, J Biomed Mat Res 39: 478.

Mamedova NN, Kotov NA, Rogach AL, Studer J (2001) Albumin-CdTe nanoparticle bioconjugates: preparation, structure, and interunit energy transfer with antenna effect, Nano Letters 1: 281.

Masuda R, Takahashi W, Ishii M (1990) Particle size distribution of spherical silica gel produced by sol-gel method, J Non-Cryst Solids 121: 389.

Matsuya T, Tashiro S, Hoshino N, Shibata N, Nagasaki Y, Kataoka K (2003) A core-shell-type fluorescent nanosphere possessing reactive poly(ethylene glycol) tethered chains for zeptomole detection of protein in time-resolved fluorometric immunoassay, Anal Chem 75: 6124.

McMillan RA, Paavola CD, Howard J, Chan SL, Zaluzec NJ, Trent JD (2002) Ordered nanoparticle arrays formed on engineered chaperonin protein templates, Nat Mater 1: 247.

Meyer C, Haase M, Hoheisel W, Bohmann K (2003) Core/shell nanoparticles suitable for (F)RET-assays, Patent WO 2004/096944 A1.

Miles LEH, Hales CN (1968) Labelled antibodies and immunological assay systems, Nature 219: 186.

Mooradian A (1969) Photoluminescence of metals, Phys Rev Lett 22: 185.

Murray CB, Kagan CR, Bawendi MG (2000) Synthesis and characterization of monodisperse nanocrystals and packed nanocrystal assemblies, Annu Rev Mater Sci 30: 545.

Murray CB, Norris DJ, Bawendi MG (1993) Synthesis and characterization of nearly monodisperse CdE (E = sulfur, selenium, tellurium) semiconductor nanocrystallites, J Am Chem Soc 115: 8706.

Narayanan SS, Sarkar R, Pal SK (2007) Structural and functional characterization of enzyme-quantum dot conjugates: covalent attachment of CdS nanocrystal to α-chymotrypsin, J Phys Chem C 111: 11539.

Niedbala RS, Feindt H, Kardos K, Vail T, Burton J, Bielska B, Li S, Milunic D, Bourdelle P, Vallejo R (2001) Detection of analytes by immunoassay using up-converting phosphor technology, Anal Biochem 293: 22.

Nirmal M, Dabbousi O, Bawendi MG, Macklin JJ, Trautman JK, Harris TD, Brus LE (1996) Fluorescence intermittency in single cadmium selenide nanocrystals, Nature 383: 802.

Näreoja T, Vehniäinen M, Lamminmäki U, Hänninen PE, Härmä H (2008) Study on nonspecificity of an immunoassay using nanoparticle labels. Unpublished manuscript.

Ohmori M, Matijevic E (1992) Preparation and properties of uniform coated colloidal particles. VII. Silica hematite, J Colloid Interface Sci 150: 594.

Oi VT, Glazer AN, Stryer L (1982) Fluorescent phycobiliprotein conjugates for analyses of cells and molecules, J Cell Biol 93: 981.

Okubo M, Azume I, Yamamoto Y (1990) Preferential adsorption of bovine serum albumin dimer onto polymer microspheres having heterogeneous surface consisting of hydrophobic and hydrophilic parts, Colloid Polym Sci 268: 598.

Olshavsky MA, Goldstein AN, Alivisatos AP (1990) Organometallic synthesis of gallium-arsenide crystallites, exhibiting quantum confinement, J Am Soc Chem 112: 9438.

Paik UG, Kim JP, Jung YS, Jung YG, Katoh T, Park JG, Hackley VA (2001) The effect of Si dissolution on the stability of silica particles and its influence on chemical mechanical polishing for interlayer dielectric, J Korean Phys Soc 39: S201.

Perrin F (1926) Polarisation de la lumière de fluorescence. Vie moyenne de molécules dans l'état excité, J Phys Radium 7: 390.

Pires AM, Serra OA, Davolos MR (2005) Morphological and luminescent studies on nanosized Er, Yb-yttrium oxide up-converter prepared from different precursors, J Luminescence 113: 174.

Plowman TE, Durstchi JD, Wang HK, Christensen DA, Herron JN, Reichert WM (1999) Multiple-analyte fluoroimmunoassay using an integrated optical waveguide sensor, Anal Chem 71: 4344.

Prat O, Lopez E, Mathis G (1991) Europium(III) cryptate: A fluorescent label for the detection of DNA hybrids on solid support, Anal Biochem 195: 283.

Putalun W, Fukuda N, Tanaka H, Shoyama Y (2004) A one-step immunochromatographic assay for detecting ginsenosides Rb1 and Rg1, Anal Bionanal Chem 378: 1338.

Pötschke K, Müller-Kirsch L, Heitz R, Sellin RL, Pohl UW, Bimberg D, Zakharov ND, Werner P (2004) Ripening of self-organized InAs quantum dots. Physica E 21: 606.

Rapino S, Zerbetto F (2007) Dynamics of Thiolate Chains on a Gold Nanoparticle, Small 3: 386.

Roberts DV, Wittmershaus BP, Zhang Y-Z, Swan S, Klinovsky MP (1998) Efficient excitation energy transfer among multiple dyes in polystyrene microspheres, J Lumin 79: 225.

Romero-Steiner S, Caba J, Rajam G, Langley T, Floyd A, Johnson SE, Sampson JS, Carlone GM, Ades E (2006) Adherence of recombinant pneumococcal surface adhesion A (rPsaA)-coated particles to human nasopharyngeal epithelial cells for the evaluation of anti-PsaA functional antibodies, Vaccine 24: 3224.

Rossi MJ, Dyer MJ, Faris GW, Kane J, Ng SY, Zarling DA, Peppers NA, Schneider LV (1997) Up-converting reporters for biological and other assays using laser excitation techiques, US Patent 5,674,698.

Rowe CA, Scruggs SB, Feldstein MJ, Golden JP, Ligler FS (1999) An assay immunosensor for simultaneous detection of clinical analytes, Anal Chem 71: 433.

Roy BC, Santos M, Mallik S, Campiglia AD (2003) Synthesis of metal-chelating lipids to sensitize lanthanide ions, J Org Chem 68: 3999.

Rundström G, Jonsson A, Mårtensson O, Mendel-Hartvig I, Venge P (2007) Lateral flow immunoassay using europium (III) chelate microparticles and time-resolved fluorescence for eosinophils and neutrophils in whole blood, Clin Chem 53: 342.

Saito K, Kobayashi D, Sasaki M, Araake H, Kida T, Yagihashi A et al. (1999) Detection of human serum tumor necrosis factor-alfa in healthy donors, using a highly sensitive immuno-PCR assay, Clin Chem 45: 665.

Santra S, Zhang P, Wang K, Tapec R, Tan W (2001) Conjugation of biomolecules with luminophore-doped silica nanoparticles for photostable biomarkers, Anal Chem 73: 4988.

Schmid G (1992) Large clusters and colloids. Metals in the embryonic state, Chem Revs 92: 1709

Schult K, Katerkamp A, Trau D, Grawe F, Cammann K, Meusel M (1999) Disposable optical sensor chip for medical diagnostics: new ways in bioanalysis, Anal Chem 71: 5430.

Seitz WR (1984) Immunoassay labels based on chemiluminescence and bioluminescence, Clin Biochem 17: 120.

Selvin PR (1995) Fluorescence resonance energy transfer, Methods Enzymol 246: 300.

Shim S-E, Cha Y-J, Byun J-M, Choe S (1999) Size control of polystyrene beads by multistage seeded emulsion polymerization, J Appl Polym Sci 71: 2259.

Shirahama H, Suzawa T (1985) Adsorption of bovine serum albumin onto styrene/acrylic acid copolymer latex, Colloid Polym Sci 263: 141.

Shirahama H, Shikuma T, Suzawa T (1989) Participation of electrolyte cations in albumin adsorption onto negatively charged polymer lattices, Colloid Polym Sci 267: 587.

Singer JM, Plotz CM (1956) The latex fixation test: I. Application to the serological diagnosis of rheumatoid arthritis, Am J Med 21: 888.

Soini E, Hemmilä I (1979) Fluoroimmunoassay: present status and key problems, Clin Chem 25: 353.

Soini E, Kojola H (1983) Time-resolved fluorometer for lanthanide chelates – a new generation of non-isotopic immunoassays, Clin Chem 29: 65.

Soini E, Lövgren T (1987) Time-resolved fluorescence of lanthanide probes and applications in biotechnology, CRC Crit Rev Anal Chem 18: 105.

Sokolov I, Klevsky Y, Kaszpurenko JM (2007) Self-assembly of ultrabright fluorescent silica particles, Small 3: 419.

Sordelet D, Akinc M (1988) Preparation of spherical monosized Y_2O_3 precursor particles, J Colloid Interface Sci 122: 47.

Soukka T, Härmä H, Paukkunen J, Lövgren T (2001a) Utilization of kinetically enhanced monovalent binding affinity by immunoassays based on multivalent nanoparticle-antibody biocinjugates, Anal Chem 73: 2254.

Soukka T, Paukkunen J, Hämä H, Lönnberg S, Lindroos H, Lövgren T (2001b) Supersensitive time-resolved immunofluorometric assay for free prostate-specific antigen with nanoparticle label technology, Clin Chem 47: 7.

Soukka T, Antonen K, Härmä H, Pelkkikangas A-M, Huhtinen P, Lövgren T (2003) Highly sensitive imunoassay of free prostate-specific antigen in serum using europium(III) nanoparticle label technology, Clin Chim Acta 328: 45.

Soukka T, Kuningas K, Rantanen T, Haaslahti V, Lövgren T (2005) Photochemical characterization of up-converting inorganic lanthanide phosphors as potential labels, J Fluor 15: 513.

Spanhel L, Haase M, Weller H, Henglein A (1987) Photochemistry of colloidal semiconductors. 20. Surface modification and stability of strong luminescing CdS particles, J Am Chem Soc 109: 5649.

Srivastava S, Verma A, Frankamp BL, Rotello VM (2005) Controlled assembly of protein-nanoparticle composites through protein surface recognition, Adv Mater 17: 617.

Stouwdam JW, Hebbink GA, Huskens J, van Weggel FCJM (2003) Lanthanide-doped nanoparticles with excellent luminescent properties in organic media, Chem Mat 15: 4604.

Stouwdam JW, Raudsepp M, van Veggel FCJM (2005) Colloidal nanoparticles of Ln^{3+}-doped $LaVO_4$: energy transfer to visible- and near-infrared-emitting lanthanide ions, Langmuir 21: 7003.

Stouwdam JW, van Veggel FCJM (2004) Improvement in the luminescence properties and processability of LaF_3/Ln and $LaPO_4$/Ln nanoparticles by surface modification, Langmuir 20: 11763.

Stryer L (1978) Fluorescence energy transfer as a spectroscopic ruler, Annu Rev Biochem 47: 819.

Stöber W, Fink A, Bohn E (1968) Controlled growth of monodisperse silica spheres in the micron size range, J Colloid Int Sci 26: 62.

Sun L, Yao J, Liu C, Liao C, Yan C (2000) Rare earth activated oxide phophors: synthesis and optical properties, J Fluorescence 87: 447.

Suzawa T, Shirahama H, Fujimoto T (1982) Adsorption of bovine serum albumin onto homo- and copolymer lattices, J Colloid Interface Sci 86: 144.

Swift JL, Cramb DT (2008) Nanoparticles as fluorescence labels: is size all that matters?, Biophys J 95: 865.

Taboada-Serrano P, Chin G-J, Yiacoumi S, Tsouris C (2005) Modeling aggregation of colloidal particles, Curr Opin Colloid Interface Sci 10: 123.

Tamaki K, Shimomura M (2002) Fabrications of luminescent polymeric nanoparticles containing lanthanide (III) ion complexes, Int J Nanosci 1: 533.

Tanke HJ, Slats JCM, Ploem JS (1986) Labeled macromolecules: a process for their preparation and their use for immunological and immunochemical assays, International Patent Application 8502187.

Taton TA, Mirkin CA, Letsinger RL (2000) Scanometric DNA array detection with nanoparticle probes, Science 289: 1757.

Templeton AC, Hostetler MJ, Kraft CT, Murray RW (1998) Reactivity of monolayer-protected gold cluster molecules: steric effects, J Am Chem Soc 120: 1906.

Tessari G, Bettinelli M, Speghini A, Ajò D, Pozza G, Depero LE, Allieri B, Sangaletti L (1999) Synthesis and optical properties of nanosized powders: lanthanide-doped Y_2O_3, Appl Surface Sci 144: 686.

Tocchetti EV, Flower RL, Lloyd JV (2001) Assessment of in vitro-generated platelet microparticles using a modified flow cytometric strategy, Thrombosis Res 103: 47.

Tomlinson S, Lyga A, Huguenel E, Dattagupta N (1988) Detection of biotinylated nucleic acid hybrids by antibody-coated gold colloid, Anal Biochem 171: 217.

Ullman A (1996) Formation and structure of self-assembled monolayers, Chem Rev 96: 1533.

Ullman EF, Kirakossian H, Switchenko AC, Ishkanian J, Ericson M, Wartchow CA, Pirio M, Pease J, Irvin BR, Singh S, Singh R, Patel R, Dafforn A, Davalian D, Skold C, Kurn N, Wagner DB (1996) Luminescent oxygen channeling assay (LOCI): sensitive, broadly applicable homogeneous immunoassay method, Clin Chem 42: 1518.

Ushida H, Curtis CJ, Nozik AJ (1991) Gallium arsenide nanocrystals prepared in quinoline, J Phys Chem 95: 5382.

Wakefield G, Keron HA, Dobson PJ, Hutchison JL (1999) Synthesis and properties of sub-50-nm europium oxide nanoparticles, J Colloid Interface Sci 215: 179.

van den Hul HJ, Vanderhoff JW (1970) Inferences on the mechanism of emulsion polymerisation of styrene from characterisation of the polymer end-groups, Brit Polym J 2: 121.

Wang X, Li K, Shi D, Xiong N, Jin X, Yi J, Bi D (2007) Development of an immunochromatographic lateral-flow test strip for rapid detection of sulfonamides in eggs and chicken muscles, J Agric Food Chem 55: 2072.

Wang X-Q, Sun P, O'Gorman M, Tai T, Paller AS (2001) Epidermal growth factor receptor glycosylation is required for ganglioside GM3 binding and GM3-mediated suppresion of activation, Glycobiology 11: 515.

Wang Y, Herron N (1991) Nanometer-sized semiconductor clusters: materials synthesis, quantum size effects, and photophysical properties, J Phys Chem 95: 525.

Van Weemen BK, Schuurs AHWM (1971) Immunoassay using antigen-enzyme conjugates, FEBS Letts 15: 232.

Weller H (1993) Colloidal semiconductor q-particles: chemistry in the transition region between solid state and molecules, Angew Chem Int Ed. 32: 41.

Welzel P (2002) Investigation of adsorption-induced structural changes of proteins at solid/liquid interfaces by differential scanning calorimetry, Thermochim Acta 382: 175.

Verheijen R, Stouten P, Cazemier G, Haasnoot W (1998) Development of a one step strip test for the detection of sulfadimidine residues, Analyst 123: 2437.

Verma A, Rotello VM (2005) Surface recognition of biomacromolecules using nanoparticle receptors, Chem Commun 3: 303.

Vertegel AA, Siegel RW, Dordick JS (2004) Silica nanoparticle size influences the structure and enzymatic activity of adsorbed lysozyme, Langmuir 20: 6800.

Werts MHV, Duin MA, Hostraat JW, Verhoeven JW (1999) Bathochromicity of Michler's ketone upon coordination with lanthanide(III) beta-diketonates enable efficient sensitization of Eu^{3+} for luminescence under visible light excitation, Chem Commun 799.

Wide L, Bennich H, Johansson SGO (1967) Diagnosis of allergy by an in-vitro test for allergen antibodies, Lancet 2: 1105.

Wilcoxon JP, Martin JE (1998) Photoluminescence from nanosize gold clusters, J Chem Phys 108: 9137.

Vogel R, Surawski PPt, Littleton BN, Miller CR, Lawrie GA, Battersby BJ, Trau M (2007) Fluorescent organosilica micro- and nanoparticles with controllable size, J Colloid Interface Sci 310: 144.

von Lode P, Hagrén V, Palenius T, Lövgren T (2003) One-step quantitative thyrotropin assay for the detection of hypothyroidism in point-of-care conditions, Clin Biochem 36: 121.

von Lode P, Rainaho J, Pettersson K (2004) Quantitative, wide-range, 5-minute point-of-care immunoassay for total human chorionic gonadotropin in whole blood, Clin Chem 50: 1026.

Wright WH, Mufti NA, Tagg NT, Webb RR, Schneider LV (1997) High-sensitivity immunoassay using a novel upconverting phosphor reporter, Proc SPIE – Int Soc Opt Eng 2985: 248.

Yamamoto Y, Tsutsumi Y, Yoshioka Y, Nishibata T, Kobayashi K, Okamoto T, Mukai Y, Shimizu T, Nakagawa S, Nagata S, Mayumi T (2003) Site-specific PEGylation of a lysine-deficient TNF-α with full bioactivity, Nat Biotechnol 21: 546.

Ye T, Zhao G, Weiping Z, Shangda X (1997) Combustion synthesis and photoluminescence of nanocrystalline Y_2O_3:Eu phosphors, Mat Res Bull 32: 501.

Ye Z, Tan M, Wang G, Yuan J (2004) Preparation, characterization, and time-resolved fluorometric application of silica-coated terbium(III) fluorescent nanoparticles, Anal Chem 76: 513.

Ylikotila J, Hellström JL, Eriksson S, Vehniäinen M, Välimaa L, Takalo H, Bereznikova A, Pettersson K (2006) Utilization of recombinant Fab fragments in a cTnI immunoassay conducted in spot wells, Clin Biochem 39: 843.

Yoon J-Y, Park H-Y, Kim J-H, Kim W-S (1996) Adsorption of BSA on highly carboxylated microspheres – quantitative effects of surface functional groups and interaction forces, J Colloid Interface Sci 177: 613.

Yoon J-Y, Kim J-H, Kim W-S (1999) The relationship of interaction forces in the protein adsorption onto polymeric microspheres, Colloids and Surfaces A: Physiochem Engin Asp 153: 413.

Zarling DA, Rossi, MJ, Peppers, NA, Kane J, Faris, GW, Dyer MJ, Ng SY, Schneider LV (1997) Up-converting reporters for biological and other assays using laser excitation techniques, US Patent 6,399,397 B1.

Zhao J, O'Daly JP, RWHJ Stonehuerner, Crumbliss AL (1996) A xanthine oxidase/colloidal gold enzyme electrode for amperometric biosensor applications, Biosens Bioelectron 11: 493.

Ziljmans HJMAA, Bonnet J, Burton J, Kardos K, Vail T, Niedbala RS, Tanke HJ (1999) Detection of cell and tissue surface antigens using up-converting phosphors: a new reporter technology, Anal Biochem 267: 30.

Zimmer JP, Kim S-W, Ohnishi S, Tanaka E, Frangioni JV, Bawendi MG (2006) Size series of small indium arsenide-zinc selenide core-shell nanocrystals and their application to in vivo imaging, J Am Chem Soc 128: 2526.